UNIVERSITÀ DEGLI STUDI DI NAPOLI FEDERICO II

Scuola di Medicina e Chirurgia

Dipartimento di Scienze Biomediche Avanzate

Sezione di Anatomia Patologica

DOTTORATO DI RICERCA IN
SCIENZE BIOMORFOLOGICHE E CHIRURGICHE
XXX Ciclo
Coordinatore Prof. Alberto Cuocolo

TESI

Prognostic role of PATZ1 protein in gliomas and its implication with stemness

TUTOR
Prof. Gaetano De Rosa

CANDIDATO
Dott.ssa Elia Guadagno

Anno accademico 2016/ 2017

INDEX

ABSTRACT. pag.3
INTRODUCTION. pag.4
1. Gliomas and oligodendogliomas. pag.4
1.1 Epidemiology and classification. pag.4
1.2 Glioblastoma IDH-wild type. pag.6
1.3 Glioblastoma IDH-mutated. pag.20
1.4 Glioblastoma NOS. pag.22
1.5 OligodendrogliomaIDH-mutatedand1p/19q codeleted, and oligodendroglioma NOS. pag.22
2. PATZ1. . . . . pag.23
2.1 PATZ1: Role in embriology. pag.23
2.2 PATZ1: Role in cancer. pag.25
2.3 PATZ1: Role in stemness. pag.28

AIMS AND SCOPES pag.34

METHODS pag.35
1.Tissuespecimens. pag.35
2. Immunohistochemicalanalysis. pag.35
3. Immunofluorescence and confocalmicroscopy. pag.36
4. Cell cultures and transfection pag.37
5. RNA extraction and quantitative real time (qRT)-PCR. pag.38
6.Protein extraction and western blot analysis. pag.38
7.Data mining. pag.39
8. Statistical analysis and Kaplan-Meier survival curves. pag.39

RESULTS pag.41
1.PATZ1 is expressed in human gliomas and is enriched in the proneuralsubtype. pag.41
2.PATZ1 is preferentially expressed in glioma stem cells. pag.49
3.PATZ1 expression levels predict survival of GBM patients. pag.51
4.PATZ1 downregulates*CXCR4* expression in GBM. pag.53

DISCUSSION. pag.55

REFERENCES pag.58

SUPPLEMENTARY MATERIAL pag.64

ABSTRACT

Glioblastoma (GBM), the most malignant of brain tumors, has been classified on the basis of molecular signature into four subtypes: classical, mesenchymal, proneural and neural, among which the mesenchymal and proneural subtypes have the shortest and longest survival, respectively. Here we show that the transcription factor PATZ1 gene is upregulated in gliomas compared to normal brain and, among GBMs, is particularly enriched in the proneural subtype and co-localize with stemnessmarkers. Accordingly, in GBM-derived glioma-initiating stem cells (GSCs) PATZ1 is overexpressed compared to differentiated tumor cells and its expression significantly correlates with the characteristic stem cell capacity to grow as neurospheres in vitro. Interestingly, survival analysis demonstrated that PATZ1 lower levels informed poor prognosis in GBM and, specifically, in the proneural subgroup, suggesting it may serve a role as diagnostic and prognostic biomarker for intra-subtype heterogeneity of proneural GBM. We also show that PATZ1 suppresses the expression of the mesenchyme-inducer CXCR4, and that PATZ1 and CXCR4 are inversely correlated in GSC and proneural GBM. Overall these findings support a central role of PATZ1 in regulating malignancy of GBM.

INTRODUCTION

1. Gliomas and oligodendrogliomas

1.1 Epidemiology and classification

Central Nervous System (CNS) tumors are relatively rare, representing 2% of all malignant tumors in the adult, while in the young age they represent the second in terms of frequency after leukemia, accounting for 20% of all neoplasms.

Diffuse astrocytic tumors (grades II-IV sec WHO) include 60% of all intracranial primitive tumors, with an annual incidence of 3.19/100,000 for glioblastomas and 0.5/100,000 people for diffuse astrocytomas, in the US population (1). In Europe, there is an average incidence of 3 cases/100,000 per year in Eastern Europe and 5/100,000 per year in the United Kingdom and Ireland (2). The country with the highest incidence of diagnosis of brain tumors is Albania, with the lowest in Cyprus (3). There is a slight predominance among males (1.3: 1) and although these can occur at any age, the risk increases substantially in the older age. Older patients are more likely to be affected by higher-grade gliomas, especially glioblastoma.

For decades, primitive CNS tumors have been classified on the basis of histological criteria by identifying tumor categories depending on their microscopic resemblance to presumed cells of origin and their degree of differentiation; tumors are classified into gliomas, meningiomas, neuronal, embryonic or poorly differentiated tumors.

Gliomas then, based on the glial cell of origin, have been classified into astrocytomas, oligodendrogliomas and ependymomas. Astrocytomas, based on their ability to infiltrate adjacent tissue and on histologic characteristics, are classified into WHO grade I (pilocyticastrocytoma) to WHO grade IV (glioblastoma) forms.

In adults, the most frequent cerebral malignant neoplasm is glioblastoma (GBM), accounting for about 15% of all intracranial tumors and 45-50% of the primitive brain tumors.

In 2016 [4], the World Health Organization drafted a new Classification of the Tumors of the CNS, which, albeit innovative in its approach, is a revision of the previous fourth edition of 2007 [5], rather than a fifth edition.

For the first time, the new classification scheme was based on the combination of histological and molecular parameters, thus providing greater objectivity for diagnosis and better understanding of tumor biology, despite, according to the current state of the art, key diagnostic criteriaare still histological.

The WHO classification system represents an evolution of the grading scheme proposed by the St. Anne and Mayo Clinic hospitals, originally formulated for needle biopsy samples and using a system based on the presence/absence of four variables: nuclear atypia, mitosis, microvascular proliferation and necrosis (Figure 1)

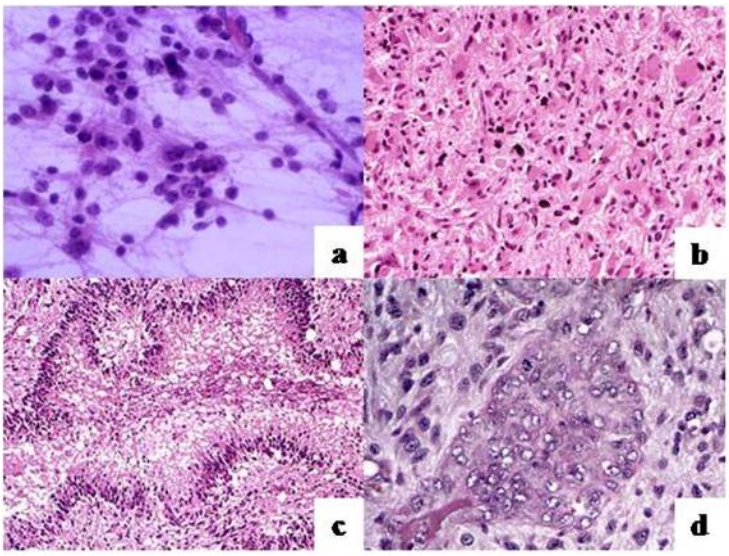

Figure 1. Four variables in the grading system according to Saint Ann-Mayo Clinic:

a. nuclear atypia; b. mitotic activity; c. pseudopalisading necrosis; d. microvascular proliferation

This new approach has allowed us to recognize new classification entities, and to abolish instead others, and has allowed to group different tumors on the basis of their clinical-pathological significance.

An example, in this sense, is represented by the category of diffuse gliomas, which group all the gliomas presenting with infiltrative characters, irrespective of their cellular origin: if, in the past, that of infiltrating astrocytoma was a separated entity from that of infiltrating oligodendroglioma, now it falls into the same category, thus encompassing WHO grade II and grade III astrocytic tumors, WHO grade II and III oligodendrogliomas, oligoastrocytomas, grade IV glioblastoma and diffusegliomas of childhood.

Within this new and large family, a key distinction is based on the search of isoenzyme dehydrogenase (IDH)mutations, allowing differentiation into IDH-mutated and IDH-wildtype tumors, depending on whether or not is present the R132H IDH1mutated protein or mutations of codon 132 for IDH1 and codon 172 for IDH2 (in clinical practice, the detection of IDH1 R132H mutation is enough to define the tumor as IDH-mutated). If it is not possible to evaluate the presence of mutations or the results are ambiguous, IDH-NOS definition (nototherwisespecified) is adopted (Figure 2).

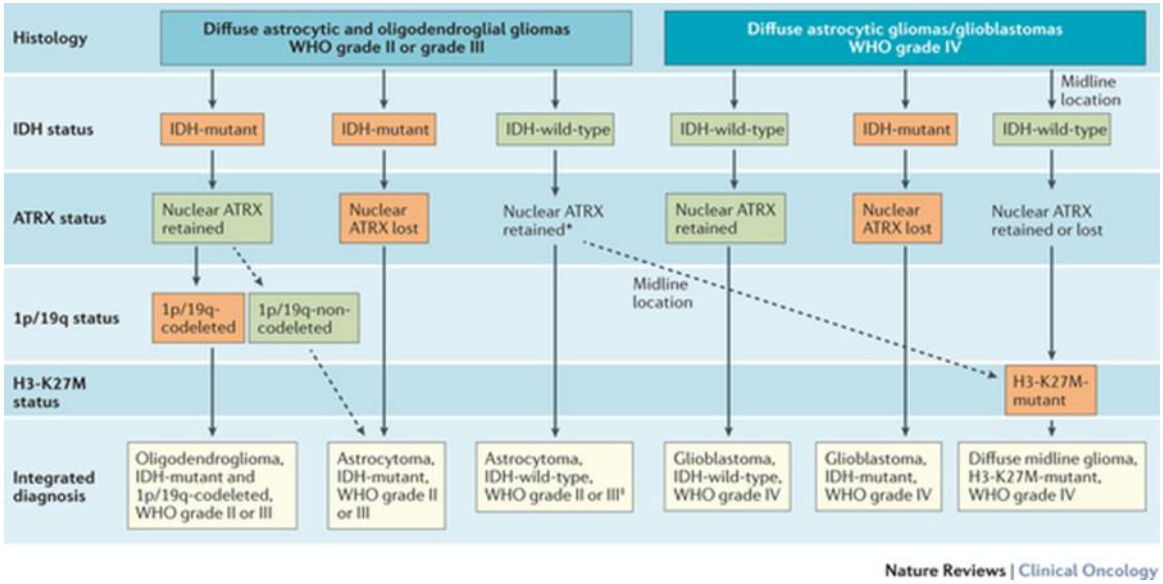

Figure 2. Diagnostic flowchart (2016 WHO)

The distinction between IDH-mutated and IDH-wildtypetumors has a predominantly prognostic value, being the prognosis of IDH-mutated glioblastomas better than the wildtype counterpart.

Further molecular aspects may be added to the determination of the IDH pattern in order to achieve a complete definition of an "integrated diagnosis".

1.2 Glioblastoma IDH-wildtype

Epidemiology and etiology

Glioblastoma IDH-wild type accounts for about 90% of all glioblastomas.

It may be defined as a high grade glioma with astrocytic predominant differentiation characterized by nuclear atypia, cell pleomorphism, high mitotic activity, diffuse growth pattern with microvascular proliferation and/or necrosis, in absence of IDH mutations. It is also named primary glioblastoma, because it originates *de novo* without progressing from a low grade lesion.

Many studies have been conducted to understand the etiology of glioblastomas without achieving univocal and definitive conclusions. Controversial is the role of non-ionizing radiations (egmobile phones) and professional exposure, while head and neck exposure toionizing radiation seems to be the only valid risk factor; conversely, a history of allergy or atopy seems to have a protective role.

Genetic susceptibility has also been demonstrated, resulting from cases of glioblastomas diagnosed in more than one member of the same family: this predisposition is due to the presence of hereditary tumor syndromes such as Type 1 Turcot syndrome, Li-Fraumeni

syndrome and type 1 neurofibromatosis. Five independent studies have then shown a fundamental role of several genes (TERT, EGFR, TP53) to increase the risk of glioblastoma.

The origin of glioblastoma is still being studied to date: if the hypothesis of dedifferentiation from astrocytic precursors is valid, the discovery of cancer stem cells that are similar to normal brain stem cells of thesubventricularzone has opened another research path [6].

Tumor stem cells are able, like all stem cells, to cause an asymmetric division, generating cells that will begin the differentiation process. It is believed that these cells are nothing but neural stem cells - as also demonstrated by the expression of CD133, Sox2, Musashi and Nestin stem cell markers. Based on the evaluation of the expressed markers, two subgroups of tumor stem cells were identified: *Type 1* cells, with proneural phenotype, resemble fetal stem cells, are CD133 and CD15 positive and have the ability to form non-adherent spheres; *Type 2* cells, with mesenchymal phenotype, are instead CD44 positive but CD133 negative, more invasive and with semi-adherent growth.

However, the presence of negativity for CD133 should not be misleading: these cells may force the classic criteria ofstemnessand give rise to positive CD133 cells; the expression of CD133 and stem behavior, therefore, must be evaluated in the light of an evolutionary process dependent also on environmental factors including the hypoxia, that is observed in stemness niches. Consequently, the use of CD133 as the sole marker of stemness and tumor aggression is unsuitable and should be evaluated in the context of the ability to form spheres and invade adjacent tissues.Since these stem cells are resistant to common therapeutic approaches and therefore responsible for disease progression, they could be used as a target for a new targeted therapy: early studies assessed the effect of an EGFR inhibitor (cetuximab) on tumor growth, focusing on vIII-EGFR mutated form, that is constitutively active and which increases proliferation by inhibiting apoptotic processes. Paradoxically, probably because an inhibitor is available, it has been shown that the presence of EGFRvIII correlates with better prognosis, while its absence is associated to resistance to standard chemotherapy. In addition, when present, EGFRvIII is mostly expressed by stem cells but not by the traditional cell lines that, once they move to the differentiation process, they quickly lose its expression.In these cases, therefore, treatment with cetuximab is completely ineffective and for this reason attention has been shifted towards signaling paths such as PI3K/Akt; CD133, in fact, forms a structural complex that stabilizes the PI3K regulatory p85 subunit on the cell membrane, contributing to increase its enzymatic activity. Subject of studies are also other tyrosine-kinase receptors such as VEGFR, PDGFR and the CXCR4 receptor for chemokines, that are crucial promoters of Proneural and Mesenchymal phenotypes.

Clinical aspects and localization

IDH-wildtype glioblastoma is generally localized in the subcortical white matter and in the gray matter of the cerebral hemispheres, involving temporal lobe in 31% of cases, parietal lobe in 24%, frontal lobe in 23% and occipital lobe in 16% of cases: it is highly probable, therefore, that the first clinical manifestation of glioblastoma is a focal neurologic deficit. In general, the tumor has a trend to infiltrate the adjacent cortex and, through the callous body, the contralateral hemisphere. The involvement of basal ganglia and thalamus is common mainly in children, whereas brainstem, cerebellum and spinal cord glioblastomas are rare.

IDH-wild type glioblastoma has rapid growth associated with edema and increased intracranial pressure which can cause nausea, vomiting, neuro-cognitive and behavioral changes, seizures and marked pulsating head pain. Generally, the average time between the onset of the first symptom and diagnosis is three months (68% of cases, 84% within six months).

Genetic profile

The evolution of normal cells to tumor cells is a multi-stage process where genetic mutations,that are progressively acquired, determine a continuum in the disease.

The most frequent chromosome abnormalities in glioblastomas are amplification of chromosome 7p (in some cases amplification may also involve chromosomes 19 and 20) and loss of chromosome 10q (less frequently also chromosomes 9 and 13).

EGFR gene is amplifiedin more than 40% of cases in primary glioblastomas and rarely in secondary forms. This amplification is often associated (25%) with a mutation of the extracellular domain of EGFR, hesitating in a constitutively activated receptor known as EGFRvIII.Tyrosine kinase-dependent signaling alterations are present in 90% of cases and, in addition to EGFR amplification, a key role is to be recognized to PDGFRα (15%), MET (5%) and mutations of FGFR1-TACC1 fusion protein. The mutation and amplification of PI3K genes (eg PIK3CA, PIK3R1) occur in less than 10% of cases, while frequently mutated (15-40%, almost exclusively in primary glioblastomas) is PTEN gene, involved in cell proliferation and in the migration and invasion mechanisms. NF1 mutations are present in approximately 20% of cases.

TP53 alterations are present in 25% of primary glioblastomas, while they reach 90% of secondary forms, wherethey are considered a distinctive and early evolutionary element, being also present in low grade lesions from which glioblastoma will evolve. In 10% of primary formswithout TP53 mutations, it is possible to identify MDM2 amplification that represents an alternative mechanism of evasion of p53-mediated cellular control.

The locus CDKN2A encodes for distinct proteins including p14ARF, which binds MDM2 and inhibits MDM2-mediated p53 degradation: loss of p14ARF expression is observed in nearly 50% of cases, as a result of the methylation of the promoter or homozygous deletion of the locus. This deletion is mutually exclusive with alterations of RB1, whose methylation of the promoter, results in its reduced expression, and appears to be more frequent in secondary glioblastomas (43%).

TERT gene promoteris mutated in about 80% of primary glioblastomas, in the absence of TP53 mutations: this alteration fails in the recruitment of a multimeric GABP protein, that behaves as a specific transcription factor for the mutated promoter, causing an aberrant expression of TERT; in secondary forms, IDH-mutated, telomere maintenance is more dependent on the mutations of ATRX and TERT genes.

IDH1 and IDH2 mutations are rare in primary glioblastoma: in case of IDH1 mutation, it is possible that glioblastoma is not really primary but resulting from a low-grade silent, undiagnosed lesion, and become apparent only in phase of progression. In primary forms, however, the mutations of the genes involved in chromatin remodeling are frequent, so that even in the absence of direct genetic alterations, epigenetic modifications may modulate gene expression. One of the fundamental functions of this regulation, in fact , is to keep intact some portions of the genome by compacting chromatin and making it inaccessible to the transcription mechanisms.Mutations of PRC2 and its catalytic subunit EZH2 are involved in this process. Another possible mechanism is silencing of DNA through the methylation of the promoters of some genes; the most frequently methylated gene (40-50%) is MGMT (O6-Methylguanine-DNA-methyltransferase), that codifies for a DNA repair protein, with a predictive role for the success of alkylating agents (temozolomide): if the promoter is hypermethylated, there will be a reduction in protein synthesis with reduced damage repair induced by chemotherapy, and hence sensitivity to treatment.

Based on the gene expression, it is possible to outline a molecular classification by identifying four subtypes of glioblastoma: classical, mesenchymal, proneural and neural [7].

Classical glioblastoma presents typical glioblastoma alterations, as amplification of chromosome 7 - also present in tumors of the other classes, in varying percentages - and loss of chromosome 10. Atypical molecular feature of this variant is the amplification of EGFR observed in 97% of cases; mutation of TP53 is almost always lacking. In 94% of cases, in association with EGFR amplification, there is homozygous focal deletion of Chr 9p21.3, centered on CDKN2A gene encoding for both p12INK4A and p14ARF; NESTIN stem cell marker is highly expressed, as well as NOTCH and Sonic-hedgehog signaling paths are activated.

In *mesenchymal* glioblastoma predominates the deletion of the 17q11.2 region containing the NF1 gene, resulting in its reduced gene expression: this condition is associated with a variety of tumors including neurofibromas, which originate from Schwann's cells and, although these cells are absent in the CNS, mesenchymal glioblastoma has its typical markers as S100A and microglia markers; frequent are the NF1/PTEN co-mutations. This variant expresses mesenchymal markers such as CHI3L1 (also known as YKL40, a glycoprotein involved in tissue remodeling, flogosis, fibrosis, asthma, and solid tumors), along with classical astrocytic markers such as CD44 and MERTK; highly expressed are the genes involved in the signaling pathways of TNF and NFKB (TRADD, RELB, TNFRSF1A).

Proneural glioblastoma shows, as peculiar aspects, the alteration of PDGRFα gene and the point mutation of IDH1; in particular, the focal amplification at locus 4q12 which results in increased PDGFRα gene expression, is found in all glioblastomas, but with higher values in the proneural variant. TP53 mutations are frequent, while classical amplification of chromosome 7, associated with loss of chromosome 10, occurs in only 54% of cases: the pattern of alterations thus constitutes the characteristic of a secondary form of glioblastoma. This variant has a high expression of oligodendrocyte development (such as NKX2-2 and OLIG2, which inhibit the oncosoppressor p21, thus favoring proliferation) and proneural genes (SOX, DCX, DLL3, ASCL1, TCF4); frequent mutations are also those involving PIK3CA/PIK3R1.

Neural glioblastoma is identified by the expression of neural markers (NEFL, GABRA1, SYT1, SLC12A5) which, together with the unequivocal aspect of optical microscopy, suggests a well-differentiated phenotype.

Such classification has proved to be of fundamental therapeutic value, as intensive radio-chemotherapy treatment with adjuvant therapy (three consecutive chemotherapy cycles) results in a confirmed reduction of mortality in classical and mesenchymal variants, only hypothetical in the neural variant and absent in the proneural. MGMT methylation state is not associated with a specific subclass.

Macroscopic and microscopic features

Despite the short time of the symptoms before the diagnosis, glioblastoma often appears as a large, infiltrating mass, occupying sometimes more than one lobe, but tendentiallymonolaterally; by the time, it begins to cross the callous body by following the myelinated fibers to extend bilaterally.

Most glioblastomas appear as an intraparenchymal lesions with epicenter into the white matter, and only rarely they are superficial and in contact with the leptomeninges and the dural

meninges: in this case, differential diagnosis with metastatic carcinoma or extra-axial lesions,such as meningioma, is essential. Infiltration of peritumoral parenchyma by single cells is almost always observed.

Glioblastoma is poorly delimited, with a variable cut surface relative to the cerebral parenchyma. The tumor mass generally appears with a central necrotic yellowish area that can occupy up to 80% of the total mass and with foci of hemorrhage, which, if extended, may cause stroke symptoms that may represent the first event of the disease; there may also be macroscopic cysts containing a turbid fluid representing necrotic liquefied tissue.

Glioblastoma of the brainstem, that is haemorrhagic and necrotic as in the supratentorial form, tends to move forward the basilar artery, extending along the fibers of the middle cerebellar peduncle; spinal glioblastoma, that is rare, is often diagnosedwhen there is alreadya significant local or distant involvement.

Microscopically, glioblastoma appears as a tumor with high cellular density, is composed by poorly differentiated and pleomorphic cells with high mitotic activity, microvascular proliferation and/or necrosis. In the past, glioblastoma was termed "multiforme" to highlight the cellular variety that can compose the tumor mass and that can cause diagnostic problems, since a biopsy obtained in stereotyping may not correspond to a valid representative sample of the entire lesion.

Besides the prevalent tumor cell type in the lesion, it is possible to identify and distinguish, cells with frankly astrocytic features. The transition between these cellular populations may be progressive or abrupt, especially if there is an emergence of a new tumor clone after acquiring further genetic mutations.

Recognizing the cell variety is important because a lesion with high polymorphism, well-defined plasma membranes, and absence of cellular processes can be exchanged for metastatic carcinoma or melanoma; sometimes, a cellularcomponent can be so predominant as to identify a specific phenotypic category of glioblastoma.

Small cell glioblastoma is characterized by small round or slightly elongated cells with hyperchromic nuclei and poor cytoplasm, nuclear atypia and intense mitotic activity. The Ki-67 proliferation index is high and with immunohistochemical approach it is possible to identify fine GFAP+ cellular processes; it is to be considered that GFAP often has cross-reactivity with keratins (antibodies CK AE1 / AE3). Positivity for nestin may be observed, as well as amplification of EGFR (70% of cases) and loss of chromosome 10 (95%); in all primary glioblastomas, instead, IDH mutations are absent.

Glioblastoma with primitive neuronal component has one or more nodules with neuronal differentiation, although most of the lesions present a typically astrocytic nature. These neuronal foci are markedly separated from the surrounding areas and exhibit increased cellularity with high nucleus/cytoplasmratio; positivity for neuronal markers (egsynaptophyses), reduction in GFAP expression, loss of long arm of chromosome 10 and an elevated Ki-67 proliferation index, comparable to that of the entire lesion, can be detected. Peculiar is the tendency to disseminate through liquor (30-40%); about one-fourth of these lesions develop from a low grade form, and is therefore classified as secondary glioblastomas, IDH-mutated.

Occasionally, glioblastomas may show anoligodendroglial component that, despite being associated with better prognosis, is not considered in the new classification as a distinct diagnostic entity. Conversely, glioblastoma with a gemystocytic component can be observed, meaning cells with short and radiated processes and with abundant non-fibrillary cytoplasm that tends to dislocate the nucleus to the periphery. Positivity for GFAP accumulates at the periphery and is lacking in the central hyaline region that is rich in intracytoplasmic organelles; in contrast, active proliferating cells exhibit a large hyperchromic nucleus with poor cytoplasm.

Giant cells, as they are usually considered a distinctive mark of glioblastoma, if predominant in the tumor mass, they may identify a giant cell glioblastoma variant that seems to be related to better prognosis: indeed, large cells are considered the effect of a regressive process rather than index of high clinical aggressiveness. This variant is characterized by a high cellular polymorphism, with lymphocytes interposed between tumor cells in a collagen and reticulin rich background; frequent are the mutations of TP53, while rare is the amplification of EGFR.

Granular cell glioblastoma is characterized by the presence of cells with granular cytoplasm that is Shiff Periodic Acid positive, which are important to be recognized because, when predominant, in rare cases, they can simulate a granular cell tumor of the pituitary gland. Another important distinction to be done is with macrophages: in a context of perivascular inflammation, in fact, tumor cells may be confused with macrophages and thus evoke a demyelinating disease rather than a neoplastic lesion, especially because the granular content can display positivity to macrophage markers such as CD68, but not for more specific markers such as CD163.

Tumor mass may also contain cells with foamy cytoplasm which are distinct from adipocytes and which, if grouped into lobules, may suggest adipose tissue; it is also possible that there are foci of glandular structures with cells with a big ovalar nucleus, with prominent nucleoli, rounded cytoplasm, low GFAP positivity, and expression of epithelial markers: in this case the definition of adenoid glioblastomas is justified. However, if there is an extensive mesenchymal

component, with expression of alpha-1-antitrypsin, actin and EMA, the diagnosis of gliosarcoma may be considered.

It is possible that cancer cells may align and accumulate in the subpial region of the cortex, in the subependimal area or around blood vessels and neurons (satellitosis): this distribution, defined as secondary structure, is the result of interaction between glioma cells and brain structures and is highly diagnostic for an infiltrating glioma.

Glioblastoma is characterized by intense mitotic activity and, despite a large intertumoral and intratumoral variability, Ki67 proliferation index is never lower than 15-20%, with possible focal values of more than 50%. The lowest degree of proliferation was found in tumors with marked gemystocyte component, although a relationship between the proliferative index and clinical outcome has not been demonstrated.

Abundant tumor vascularization is due to mechanisms of involvement of preexisting vascular, budding angiogenesis from existing vessels and vasculogenesis through recall of bone marrow cells. The basic element behind the angiogenesis is hypoxia which, through Hypoxia-Induced Factor 1-alpha (HIF1α), determines the activation of over 100 hypoxia-regulated genes, including angiogenesis-controlling proteins (VEGFA, which is the most important mediator, angiopoietin, IL8), cellular metabolism (carbon dioxide, lactate dehydrogenase), survival and apoptosis and migration (CXCR4). In this process of vascular remodeling also pericytes and cells derived from the bone marrow are involved .

Two different patterns of microvascular proliferation can be identified: glomeruloid body and endothelial hyperplasia.

The glomeruloid body is so named because of its resemblance to a glomerulus, given by mitotically active endothelial cells arranged in multiple layers together with smooth muscle cells/pericytes. This proliferation is much more marked nearby the necrosis, and is oriented towards it in response to factors released by ischemic tumor cells. A common feature is vascular thrombosis, responsible for the so-called "black veins" and involved in the ischemia of tumor tissue. Proliferating endothelial cells are positive for CD31, CD34 and VEGFR2, but negative for SMA (smooth muscle actin), and are surrounded by basal lamina and an incomplete pericytic layer, that is negative for CD31 and CD34 and positive for SMA and PDGFRB.

The second type of vascular proliferation is the so-called hyperplasia or endothelial, intraluminal proliferation, with endothelial cells inside small and medium caliber vessels (not necessarily microvascular), resulting in a single reduced or even obliterated lumen; albeit more rare, this variant has a major prognostic meaning, correlating with a worse prognosis.

Alongside vascular proliferation, necrosis is the other essential aspect of glioblastomas and its presence is one of the most important predictors of aggressive behavior. It is highlighted by neuroimaging techniques as a hypodense nucleus within a contrasting enhancing region and can occupy up to 80% of the tumor mass: the greater the necrotic portion, the less the survival. Tumor cells are collected along the margins of necrotic lesions producing a clinically defined palisading appearance.In the past, it was named “pseudopalisading”, to point out how tumor cells did not aggregate around the necrotic region but were the remains of a tumor mass that went to central necrotic degeneration. Recent studies, based primarily on HIF1α expression evaluation and other hypoxia-induced factors, have shown that tumor cells are actually actively migrating around the necrotic region, driven mainly by the hypoxic environment that is emerging: in this pattern, therefore, vascular invasion by tumor cells results in thrombotic phenomena,causing necrosis and tissue hypoxia that makes tumor cells migrate to the periphery of the necrotic region by releasing hypoxia-induced angiogenetic factors that determine microvascular proliferation, present throughout the injury, but much more evident especially in its periphery.

This high cellular and abnormal external region corresponds to the contrast enhancing ring region seen at the MRI (magnetic resonance imaging) and represents an appropriate target for the lesion sampling.

In the context of tumor lesion, there are also inflammatory cells, especially in the glioblastoma showing marked gemystocytic component. The most represented cells are microglia cells and CD8 + T lymphocytes, followed by CD4 +T lymphocytes and B lymphocytes, identifiable in less than 10% of cases; it has also been shown that a massive infiltrate of T CD8 + lymphocytes is more frequent in patients with higher survival.

Differential diagnosis

Neoplastic diagnosis is based on the recognition of cell number and atypia, such as nuclear pleomorphism or hyperchromasia, p53 proteinimmunodetection, immunohistochemicalevaluation of mutated EGFRvIII, and the search for characteristic chromosomal losses and of EGFR amplification.

Once established to be frankly neoplastic tissue, it is necessary to determine whether it is a primary form or a metastasis: metastatic tumors evolve from the stage of large-scale tumor microemboli that dislocate more than infiltrate brain tissue, unlike the obvious infiltrating nature of a glioblastoma, especially in the periphery; however, it is not to be excluded a priori that a metastasis can follow the course of the vessels and infiltrate the parenchyma by

simulating a glioma: in this case infiltration is generally limited and not widespread. Reactive astrocytes, moreover, are less frequently incorporated into the substance of a metastasis in which, generally, necrosis tends to save the vessels. Also useful are the cytological features that are typical of a glioblastoma, such as the presence of small, slightly differentiated or distinct astrocytic cells with little or no tendency to nuclear remodeling, small nucleoli and cellular and nuclear pleomorphism. Small cells of a glioblastoma are often smaller than those of a small cell carcinoma, and are found on a finely fibrillated background composed of neoplastic cellular processes blended with residues of white matter.

Within primitive CNS tumors, it is important to differentiate between glioblastomas and ependymomas (often positive for EMA), oligodendrogliomas (if anaplastic can simulate a glioblastoma), pilocytic astrocytoma and pleomorphic xantoastrocytomas (cellular pleomorphism is often considered an anaplasic indicator): it is the response of cells that at least partially retain the characteristics of the starting cells to allow adequate differential diagnosis, in addition to a valid immunohistochemical evaluation.

Finally, it is important to differentiate diagnosis from a primitive CNS lymphoma, especially in elderly patients with intracerebral invasive contrast enhancing mass: it is likely that it is a lymphoma in the case that the mass captures the contrast in a homogeneous and non-homogeneous form or with the presence of a ring of glioblastoma for the absence of central necrosis (except for patients with AIDS). Microscopically, lymphoma consistsof irregular angiocentrichypercellularity, with marked reactive gliosis, apoptosis, and lack of microvascular proliferation; it is composed of not cohesive, round, or reniform cells with poor cytoplasm, vesicular nuclei, with evident chromatin and nucleoli.

Diffusion and metastasis

Infiltrating growth is one of the fundamental aspects for the definition of diffuse gliomas and, above all, glioblastoma is characterized by a rapid invasion of adjacent brain structures.

Generally, the tumor moves along the white matter, although it is not uncommon to involve the cortex or deep gray matter: when the growth follows the callous body, and then extends into the contralateral hemisphere, a symmetric lesion is formed and it is defined as "butterfly glioblastoma". Likewise, the tumor may spread through the fornix, the anterior commissure or the optical radiations, resulting in perivascular aggregates, subpial dissemination and perineuronalsatellitosis, which form Scherer's secondary structures.

Infiltration tends to extend with a decreasing gradient of cell density starting from the center of the tumor, and it is possible to identify,by microscopy, single cell that stands even several

centimeters from the major lesion, both in hyperintense regions in T2 to RM and in regions that appear not to be involved by the disease in imaging: these cells are often the starting point of a recurrence after therapy, either because they escape the targeted resection and radiotherapy, or because they are located in regions where the haematopoietic barrier remains intact and thus reducing the bioavailability of drugs; it seems, however, that the activation of a transcriptional migration program is associated with a proliferation reduction.

Many glioblastomas at the onset may exhibit a typical growth pattern of *gliomatosiscerebri* which, despite being deleted as a clinical entity by the WHO 2016 classification, is still considered a typical growth variant of diffuse gliomas, with frankly neoplastic and aggressive astrocytomas inside intact brain areas that may be within the same hemisphere (with involvement of at least three lobes) or both cerebral hemispheres until reaching the deep gray matter, the brainstem, the cerebellum and the spinal cord.

Mechanisms underlying the invasiveness of glioblastomas involve cellular motility, cell-cell and cell-matrix interactions, and extracellular matrix remodeling. In fact, tumor cells are able to secrete invasion-promoting proteolytic enzymes such as the MMP2 and MMP9 matrix metalloproteinases, uPA and its uPAR receptor, and catepsins, as well as integrin receptors that mediate interaction with molecules of extracellular space, causing changes in the cytoskeleton and activation of intracellular signaling pathways such as AKT, mTOR and MAPK; in this regard, the existence of "adaptive proteins", including Pinch, has been shown to catalyze these interactions by providing all of the protein structures in the directions in which the contact is most likely to occur, thus accelerating the processes of signal transduction.

Migration is also favored by growth factors expressed by glioblastoma cells, including hepatic, fibroblastic, epidermal and endothelial growth factors; cells with EGFR amplification are usually located at the apex of the infiltrated portions, suggesting a key role in peripheral expansion.

Tumor expansion moves radially from the center of the lesion, that is necrotic and hypoxic, and hypoxia activating factors such as HIF1-alpha helps this migration: hypoxic cells show an increase in intracellular protein associated with motility and greater interaction with the extracellular matrix. In terms of motility, it is essential that cells adhere to the stroma and carry the entire body of the cell: this movement is guaranteed by prolongations called "filopods", highly augmented in the tumors, which increase the ability to adhere and drag the cell body; fascin protein is involved in this process, inducing the formation of actin filaments within these cellular protrusions, so as to make these prolongations more robust.

Despite this rapid infiltrating growth, however, glioblastoma rarely invades the subarachnoidal space or spreads through the liquor; similarly, rare is the invasion of the dura, the veins and the bone. At vascular level, tumor cells tend to adhere around the vessels, without entering them. Recently, however, cancer cells circulating in the blood have been identified, unable to give metastasis because of the optimal immune system and because of themicroenvironment ofdistant organs that is inadequate and can inhibit cell growth and implant.Extracranial cancer detection is unusual in patients who did not have surgery.

Prognosis and Therapy

Glioblastoma is atumor with poor prognosis: most patients die within 15 to 18 months of diagnosis, less than 5% survive to five years.

Young age (<50 years) and complete macroscopic resection of the tumor are associated with longer survival, as well as MGMT promoter methylation and IDH mutation.

About the age, several trials have shown that younger patients show longer survival, also because of a wider therapeutic choice than in elderly subjects, where it is greatly influenced by potential comorbidities; to date, however, it is not possible to identify a valid cut-off to guide the clinical-therapeutic choice.

MGMT promoter methylation is a key predictor of efficacy and response to alkylation: up to 90% of long-surviving patients have a mutation in this regard; it is interesting to note how the percentage of mutations is not influenced by age.

IDH1 and IDH2 mutations, albeit associated with secondary glioblastoma, are positive prognostic factors; uncertain is the role of p53 mutation, which in some studies resulted to be correlated with increased survival, whereas in others it did not show any prognostic significance; the correlation between EGFR amplification and survival is demonstrated (it is hypothesized that it may be prognostically unfavorable only if associated with p53 wild-type). Some studies have associated the loss of long arm of chromosome 10 to a lesser survival, while the correlation between PTEN mutation and prognosis is unclear.

Histologically, the microscopic aspect of the tumor typically does not give any significant prognostic implications: an exception, still to be validated, would be for giant cell glioblastoma, correlated with a better prognosis than other forms of glioblastoma, especially if considered as a regressive form.

A significant tribute to poor prognosis of glioblastoma is high resistance to standard therapy that provide a slightincrease of survival despite aggressive tumor resection, and that consists of

temozolomide chemotherapy, focal radiotherapy (with maximum dose directed to the region of contrast enhancing in MRI) and subsequent adjuvant chemotherapy at the maximum tolerated dose. This resistance is determined by a number of factors, including the presence of a blood-brain barrier, that can significantly reduce the bioavailability of drugs at the brain, along with high interstitial pressure in tumor tissue that contrasts drugs diffusion.

Besides this, there is tendency to invasion by cancer cells, that can thus spread at distance inside the CNS, remaining within the hemato-encephalic barrier and being consequently protected; the persistence of DNA repair mechanisms (such as mismatchrepair or excisionrepair base) that reduce the effectiveness of radiotherapy and chemotherapy; intratumoral heterogeneity and genetic instability that hesitate in populations of cells resistant to multiple therapeutic approaches; the presence of a stem-like cell compartment potentially retaining resistance mechanisms other than those of the remaining tumor mass and which may contribute to therapeutic failure; genetic alterations caused by the therapeutic treatment itself or by tumor progression.

Molecular alterations are responsible for specific mechanisms of resistance or susceptibility: p53 inactivation causes defects of apoptosis, as well as mutations of the protein associated with retinoblastoma Rb1 result in an ineffective cell cycle arrest. RAS point mutations, albeit rare in glioblastoma, are critical because RAS mediated signaling pathways are activated by EGFR, PDGFR, and by IGF1 insulin-like growth factor receptor. Downstream mutations, such as a silencing of the oncosoppressorNF1 gene, may trigger the RAS pathway, causing an unregulated cell proliferation.

Similarly, abnormal activation of PDGF, IGF1 and epidermal growth factor signaling pathways, as well as alterations downstream to PTEN gene, may activate the PI3K circuit. Knowledge of these anomalies, coupled with the complete identification of all genetic changes in glioblastoma progression, has proved to be crucial to hypothesize a targeted therapeutic approach using a single signaling inhibitor.

The recent identification of a stem-like cell population has added new difficulties in treating this tumor, as these highly tumorigenic cells in immunodepressive mice are capable of overcoming the classic therapeutic schemes: the addition to therapy of bevacizumab anti-VEGF antibody has, however, presented an encouraging response rate in 65% of cases. An additional problem for this cell population is given by the radio-resistance mechanisms, with the activation of DNA damage repair that is greater than the surrounding tumor mass.Thus, resistance of glioblastomas to therapy is partially dependent on stem cell compartment on which the radio-chemotherapy combined approach is failing and consequently the cells, remaining vital, can lead

to recurrence. Promising results in this regard are from the study of bone morphogenetic protein 4 (BMP4): in vitro, this factor is able to block the proliferation of CD133-positive cells, and in vivo it can reduce tumor growth, thus acting as a negative regulator; it is assumed to be employed in association with the standard therapeutic approach.

Radiotherapy in many cases may delay the enlargement of glioblastoma, resulting in a transient phase of quiescence or remission, as evidenced by the stability or regression of neurological deficits, and by the reduction of the MRI contrast enhancing mass; in some patients, however, the tumor progresses without being affected by the treatment.

The tumor, after radiotherapy, shows low cellularity, with abundant pleomorphic astrocytes that can be both normal and cancer cells with atypia induced by radiotherapy; sometimes there are small cells with hyperchromic nuclei and poor cytoplasm whose meaning is unknown. The surrounding cerebral parenchyma, after irradiation of the tumor, shows foci of coagulative necrosis that can be distinguished from tumor necrosis using PET with fluorescence-glucose: tumor necrosis, in fact, is metabolically active or "hot", while radionecrosis has no metabolic activity ("cold"); it is also possible to identify fibrinogenic necrosis and vascular thickening that, when present in the tumor site, represent the desired and desirable effect of the therapy.

A sample of irradiated brain tissue can therefore present reactive gliosis, radio-induced necrosis, quiescent or active tumor areas: if there is evidence of mitotic activity, it can be concluded that the cellular population is in a quiescent phase of growth; if, on the contrary, there is a high Ki-67 proliferation index associated with necrosis, pseudopalisading, and microvascular proliferation, then the lesion may be both active, and therefore not responsive to therapy, and re-activated.

1.3 Glioblastoma IDH-mutated

Epidemiology and clinical features

IDH-mutated glioblastoma is defined as a high grade glioma with predominant astrocytic differentiation characterized by nuclear atypia, cell pleomorphism, high mitotic activity, widespread growth pattern with microvascular proliferation and/or necrosis, in the presence of IDH1 or IDH2 genes mutations. It is also called secondary glioblastoma [4].

It accounts for about 10% of all glioblastomas, with onset in younger patients (44 years) than those diagnosed with primary glioblastoma (62 years); male/female ratio is significantly lower than that seen for primary glioblastoma, equal to 1.05: 1 versus 1.42: 1. Different is also the

duration of clinical history, equal to 30 months in IDH-mutated forms and less than 15 months in IDH-wildtype forms.

In contrast to IDH-wild type glioblastoma, which has a diffuse distribution along the anatomic pathways, secondary IDH mutated variant shows predominant involvement of the frontal lobe, particularly of the region surrounding the rostral extension of the lateral ventricles; this location reflects the preferred location for example of the diffused IDH-mutated WHO II astrocytoma, supporting the hypothesis that there is an evolution from a low grade lesion.

Genetic profile

The fundamental and characteristic genetic characteristics of secondary glioblastoma are IDH mutations associated with a hypermethylated phenotype, alterations already identifiable in low grade lesion, along with TP53 and ATRX mutations and long arm loss of chromosome 10.

IDH mutations were first described in 2008 as those "mutations in most young patients with secondary glioblastoma associated with an increase in overall survival". It is therefore possible to consider these mutations as a molecular diagnostic marker and at the same time prognostic, fundamental in the characterization of the glioblastoma variant.

The most common IDH1 mutation is R132H (CGT → CAT), found in 91% of cases, followed by rarer mutations such as R132C (CGT → TGT, 3.6-4.6% of cases), R132G (0, 6-3.8%), R132S (0.8-2.5%) and R132L (0.5-4.4%). IDH2 gene codifies for the only human protein that is homologous to IDH1, which uses NADP+ as an electron acceptor; IDH2 mutations are rare and localized on residual R172 (R172K), which is the analogue of IDH1 R132 residual, located in the active site of the enzyme, where it forms hydrogen bonds with the isocitrate, representing its substrate.

Based on these considerations, a glioblastoma to be defined as IDH-mutated should be tested by searching for IDH1 mutation R132H and other IDH1 mutations on codon 132 and IDH2 on codon 172; in clinical practice, however, it is often sufficient the immunohistochemical evaluation ofR132 codon in the search for the most frequent mutation, R132H, using an antibody that is addressed to the gene product: if mutation is present, it is referred to as IDH-mutated form. It has been shown that, in the absence of an IDH1 R132H mutation, the probability of an alternative IDH mutation is less than 1% in patients over 54 years of age. In this case, in absence of IDH1 immunoreactivity, a diagnosis of IDH- wild type glioblastoma can be performed.

Over 90% of IDH mutated glioblastomas exhibit a proneuralmolecular expression profile, and about 30% of glioblastomas classified as proneural have been shown to be IDH-mutated.

Conversely, IDH-wild-type glioblastomas exhibit significant variability in molecular expression patterns.

A fundamental difference between the two categories of glioblastomas seems to be related to the origin cells: in addition to the presence/absence of IDH mutations, the difference in age and sex of onset, together with the different localization within the brain structure, suggests that wildtype glioblastoma cells of origin have a greater tendency to disseminate than those of the IDH mutated variant that instead tend to originate or migrate to the frontal region; recent studies have also shown that CD133 expression is higher in primary glioblastoma cells and associated with the formation of neurospheres only in IDH-wild type tumor forms.

Prognosis

Already in 1940, H.J. Scherer, a pioneer in the field of glioblastoma research, stated that "from a biological and clinical standpoint, a secondary glioblastoma that originates from a low grade lesion should be distinguished from a primary tumor and presumably represents what is in the literature defined as a glioblastoma with a long clinical history " . This observation was confirmed by subsequent studies in which the different duration of clinical history in the two forms (4 months versus 15 months) was highlighted, in addition to the different outcomes in terms of therapeutic approach: a combined approach with radiotherapy and surgery, in fact, guarantees a survival of 9.9 months in primary and 24 months in secondary variants; if adjuvant treatment with chemotherapy is also added, it reaches 15 months in primary and 31 months in secondary.

1.4 Glioblastoma NOS

NOS (not otherwise specified) glioblastoma is defined as a high grade glioma with a predominant astrocytic differentiation characterized by nuclear atypia, cell pleomorphism, high mitotic activity, widespread growth pattern with microvascular proliferation and/or necrosis, without determination of the status of genetic mutations IDH1 or IDH2.

1.5 Oligodendroglioma, IDH-mutant and 1p / 19q-codeleted and oligodendroglioma, NOS

The diagnosis of oligodendroglioma and anaplastic oligodendroglioma requires demonstration of both IDH gene family mutation and the combined loss of the entire chromosomal arms 1p and 19q (coding 1p / 19q). In the absence of immunohistochemical positivity for the R132H

mutation of the IDH1 gene, it is recommended sequencing the codon 132 of the IDH1 gene and codon 172 of the IDH2 gene. In case of non-availability of these tests or in a context of inconclusive genetic results, a histologically typical oligodendroglioma form should be named NOS. In case of anaplastic oligodendroglioma,if genetic diagnostic results are absent, the presence of genetic features that are typical of glioblastoma must be excluded [4].

Oligodendroglioma cells (Figure 3) typically show round, regular and monotone nuclei with a well-defined nuclear membrane and a very slight cellular variability. The cytoplasm tends to bulge during formalin fixation and paraffin inclusions, giving rise to cells with well-defined cell membranes, clarification of the cytoplasm and a central spherical nucleus, a combination of factors that give rise to the classic "fried egg-like" appearance.

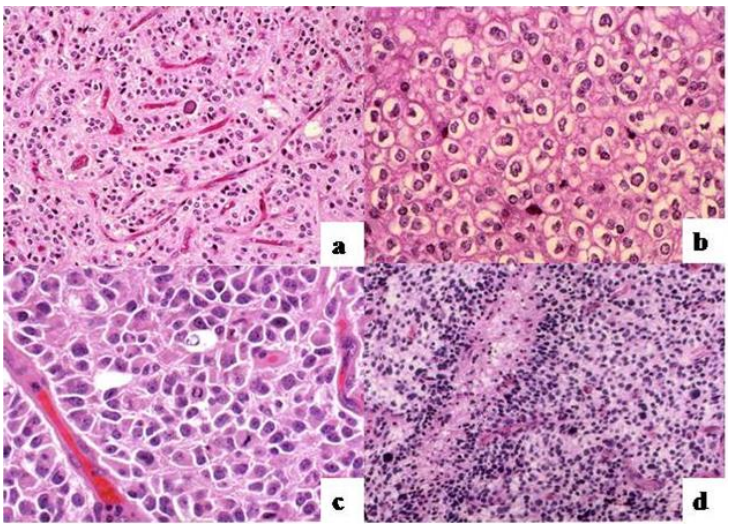

Figure 3. Oligodendroglioma: morphologic features

Grade II: a. delicate "chicken-wire" network of branching capillaries; b. typical "fried egg" pattern of cytoplasm;

Grade III: c. evident mitotic activity; d. ipercellularity.

PATZ1 (POZ/BTB and AT-hook-containing zinc finger protein 1), also known as ZNF278 (zinc finger protein 278), MAZR (MAZ-related factor) or ZSG (zinc finger sarcoma gene),is a "presumed" transcription regulator, composed of 7 zinc finger domains (Cys2-His2 type). *PATZ1* gene codes for 4 alternative proteins (from 53 to 687-amino acids long) and maps to chromosome 22q12 [8].

The knowledge of factors that are implicated in the regulation of gene expression that takes place according to a mechanism that is time-and tissue-specific, is still now subject to scientific fervor. Transcription factors have a prominent role and, as modulating proteins, they may be

classified according to the structure of their DNA-binding domain. One of these is the zinc finger domain, so named because of its link to the zinc, and of its likeness with Kruppel protein, a protein of segmentation in *Drosophila*.It is 25-30 amino acids long and it represents one of the commonest form of DNA-binding proteins [9].

Broad Complex, Tramtrack and Bric à brac (BTB) domain, also known as *Poxviruses and Zinc finger* (POZ), is a protein-protein interaction domain, which has been preserved in evolution. Originally, the members of POZ family were all transcriptional repressors, with a role in the embryological development of *Drosophila*.*Broad Complex* factors are essential for metamorphosis of *Drosophila*and their mutations cause severe impairment of the central nervous system after hormonal stimulation [10,11]; *Tramtrack* is a key regulator in the ocular development and the ablation of one or both *ttk* isoforms causes ocular alterations; finally, *Bric à brac*(Bab) rules the morphogenesis of the ovaries and the limbs [12]. All these findings involving the *Drosophila* have been the starting point for the search of a developmental role of POZ factors also in vertebrates.

Peculiar featuresof PATZ1 protein is the concomitant presence of POZ domain at N-terminal end, AT-hook domain in the center, and 4-7 zinc finger C2H2 domains at the C-terminal end (Figure4).

2.1 Role in embryology

The role of PATZ1 in embryonic development has been investigated in mice. Using experiments on "null" embryos for PATZ1, which is rendered naked for expression of PATZ1, a normal mouse embryo was compared. The group of Fedele [13] followed the embryos with in situ hybridization, between 8.5 and 17.5 days post coitum (dpc), during which the most critical phases of organogenesis take place. In general, the expression of PATZ1 is ubiquitous in the early stages of development and becomes much narrower in the later phases. The expression of this protein is much stronger in the central nervous system until it is confined in the final stages, predominantly to the proliferating neuroblasts of the periventricular areas, but also in the telencephalus (cortical plate, hippocampus, striatal neuroepithelium and the subventricular area). In the intermediate gestation phase, a strong expression was observed at the level of the olfactory and respiratory epithelium of the nasal cavities, in the retina, in the Rathke's cleft cyst, thymus, thyroid, salivary glands and dental precursors.

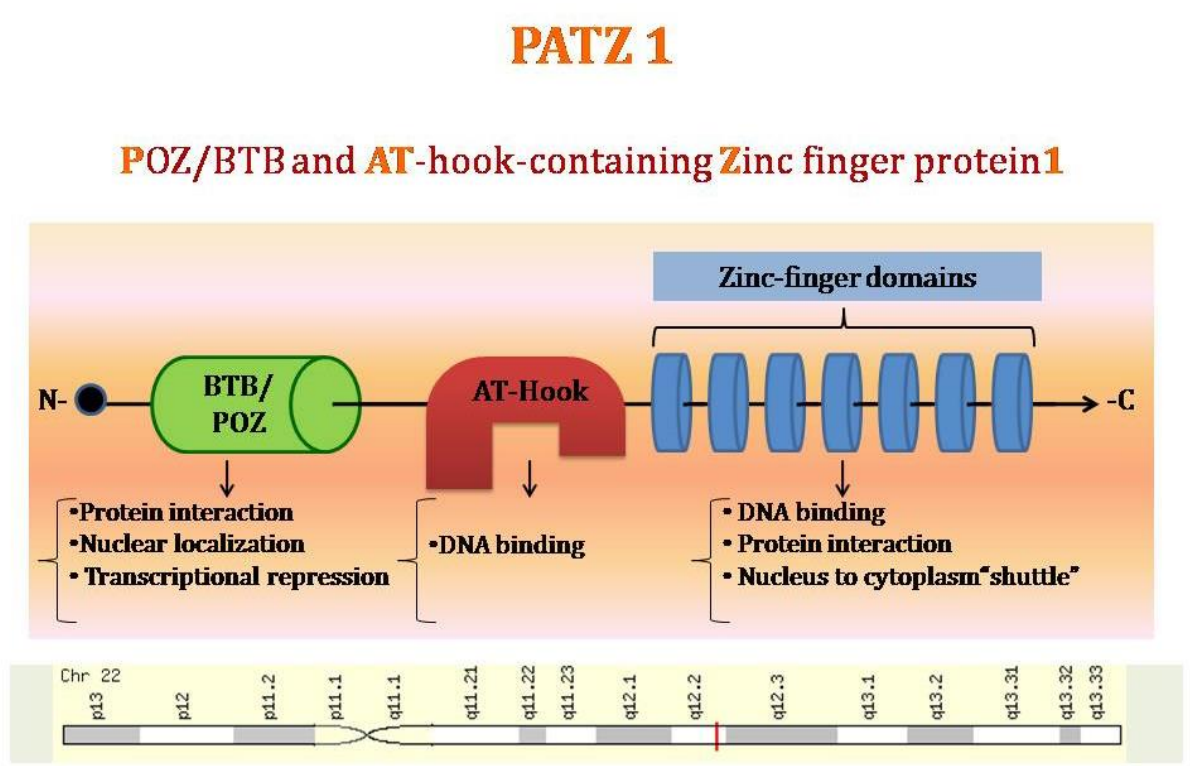

Figure 4. Structure of PATZ1 protein

In mice with homozygous mutation, it was observed a slight growth delay (the mean body weight was 10-20% less than wt mice) for gestational age and esencephaly in a percentage of cases. Esencephaly is a neural tube defect caused by deficient closure of neural folds during neurulization; where this defect is not present, however, other cerebral abnormalities are observed in homozygous mutants: the whole encephalus is smaller, the ventricular system is larger, periventricular structures are thinner, particularly at the level of thetelencephalus and diencephalusandchoroid plexus of the IV ventricle is hypoplasic.

Homozygous mutation is, in a large percentage of cases, lethal: from the mating of heterozygous mice, the percentage of living homozygous mice recorded by experiments is 4% versus 25% expected. Many of the deaths of these embryos are to be attributed to outbreaks of cardiac output defects. The prevalent expression of PATZ1 in the mesencephalus had already been observed in previously published data [14], as well as its membership of a group of candidate genes susceptible to alcoholic fetal syndrome, characterized by defects in the development of the central nervous system [15].

PATZ1 also has a critical role in spermatogenesis [16], in fact, it was seen that male null mice (- ;-) were infertile: the testis of these mice hadsmaller weight and size than the average.

Histological examination revealed the presence of semen tubules with a lower diameter and characterized by an interstitial tissue growth, containing hyperplastic Leydig cells. The most characteristic aspect to be observed was the blockage of spermatogenesis; most ofthetubules appearedcystically dilated, with loss of cellular component. Many tubules, in fact, contained only Sertoli cells and few spermatogons, other contained Sertoli cells, spermatogons in degeneration, and rare spermatocytes. Infertility was to be attributed to the absence of spermatids and spermatozoa. In association with impaired spermatogenensis, an increase of apoptosis was observed, resulting in a loss of tubular structures.

Expression analysis of PATZ1 in the normal testicle, using Northern blot, western blot and immunohistochemical techniques, revealed its presence in Sertoli cells, in a few Leydig cells and, among germ cells, exclusively in spermatogons.

The expression of PATZ1 was also studied, using total RNA in wild-type mice at different ages and it was seen to be maximum at 6 days when the germ cell count is rich in spermatogenes, still present at 13 days when spermatocytes are observed, and it is very low at 34 days when spermatocytes and spermatids are present.

All of these observations lead to the conclusion that PATZ1 protein plays an important role in the development of the testicle, by attenuating the activity of the androgenic co-regulator RNF4. Although it is unclear whether AR is expressed in germ cells, spermatogenesis is essentially dependent on androgen action, of which Sertoli's cells may be the source. Another important observation is that PATZ1 is expressed essentially by spermatogons, where it plays a role in repressing the transcription, in order to maintain stem cell pool.

2.2 Role in cancer

The first description of the association between PATZ1 and cancer dates back to 2000, when an Italian group [17] identified, in the small cell tumors, the existence of fusion between EWS and a new gene coding for a zinc finger (ZSG , Zinc finger Sarcoma Gene). It is well known that the family of cancers to which belongs Ewing's sarcoma and small cell tumors, is often carrier of translocation between the EWS gene, mapping on chromosome 22 (22q12), and different types of genes, mapping on different chromosomes and encoding DNA binding proteins (FLI1, ERG, ETV1, etc.), giving rise to tumors with distinct phenotypes (clear cell sarcomas, small cell desmoplastic tumors, mixoidliposarcoma, etc.). The EWS gene is, by definition, a "promiscuous partner". The peculiarity of the discovery was that the gene of the "zinc finger" protein identified in this study, subsequently better encoded and named PATZ1, mapped precisely on Chr22q12: for the first time it was described an intra-chromosomic rearrangement not detectable by

cytogenetic techniques, activating the EWS gene, in a case of Ewing's sarcoma,with t(1; 22) (q36.1; q12) type translocation.

The rearrangement concerns EWS intron8 and ZSG exon1, by creating a chimeric sequence containing the fusion between the EWS transactivation domain and ZSG zinc finger domain. The latter, therefore, lacking the transcriptional repressor domain at the N-terminal end (POZ domain), becomes an activator, responsible, probably, of neoplastic stimulation. The close resemblance of this protein with other proteins of the same family, with oncogenic function (PLZF, involved in acute promielocytic leukemia and BCL6, in non-Hodgkin's large B cell lymphomas), encouraged the search for its possible role in cancerogenesis.

Another oncological field where PATZ1 action has been explored is that of the glioma. Experiments were doneon [18] glioma cell cultures expressing PATZ1 mRNA, which were resistant to apoptosis induced by Fas-L, and an increase in apoptosis induced by FasL after stimulation with actinomycin D was observed. Apoptosis is an active cell death process, operating under normal and pathological conditions and it may be induced by a large number of unrelated stimuli. Fas (CD95) and its ligand (FasL) are members of the TNF receptor family and their binding triggers the death of cells expressing the receptor. Many neoplastic cells, including those of glioma, express these proteins and can be resistant to death induced by this link [19-21]. It is also known that FasL expression is a mechanism by which neoplastic cells escape immunosurveillance.

Several mechanisms are described through which glioma cells resist Fas-induced death [22,23]. Characterized by great genetic instability, glioma cells, through genetic and epigenetic alterations, are able to choose between different mechanisms of resistance, (severe "mutant phenotype")[24].

PATZ1 mRNA is expressed in brain tissue, without any differences between normal and tumor and, as mentioned above, although not implicated directly in the molecular cascade of apoptosis, the testis seems to play an important role in spermatogenesis: its shutdown causes an increase in apoptotic activity within semen tubules.

Similarly, in glioma cells, PATZ1 gene has been down-regulated by the use of a specific siRNA (small interfering RNA or silencing RNA, a RNA molecule with a length of 19-21 nucleotides, with the function of inhibiting the expression of individual genes), and it was observed that in cultures with resistance to apoptosis induced by FasL, there was an increase in cells in apoptosis and a reduction in the percentage of vital cells. PATZ1 down regulation would also increase the

sensitivity of glioma cells to apoptosis induced by mechanisms other than Fas (TRAIL, whose receptor is DR5).

The final effect of PATZ1 on cellular lines of glioma is therefore the increase of apoptosis and the reduction of proliferative activity;these results are encouraging for the detection of a specific siRNAdirected to PATZ1 as a therapeutic agent for the treatment of gliomas.

As for the testicle, the same working group [16] that evaluated the protein's immunohistochemical expression in normal tissue also did it in samples from testicular germ cell tumors, of both seminomatous and non-seminomatous type. In particular, it was observed that PATZ1 expression is greater in the cytoplasm rather than in the nucleus in both tumor types; moreover, all in situ carcinomas expressed the protein. These results, that were confirmed by western blot analysis, were in contrast to what was known until then. Since PATZ1 belongs to a family of repressor factors, it has been suggested to include it among proteins with oncosoppressor role. In testicular tumors, this observation proved to be ineffective if we consider that the protein is hyperexpressed, but still valid if we consider that in these tumors it is delocalized in the cytoplasm.

At the same time, it was argued that the cytoplasmic sequestration of nuclear proteins is a mechanism through which cancer cells promote carcinogenicity in human [24,25]. As a result, a question was unanswered: does cytoplasmic delocalization contribute to the abolition of its original function (repression) or to the acquisition of a new function in the cytoplasm?

Extremely alien to the previously acquired knowledge, it is the study of the role of PATZ1 in colon cancer. The transcriptional level of the protein was evaluated [26]via RT-PCR, finding an increase in tumor samplescompared to normal tissue. To study the function of "zinc finger" protein in this category of carcinoma, a cell line of colorectal carcinoma, with PATZ1 over-expression, was created and then transfected with siRNA directed against PATZ1. Down-regulation of this gene resulted in a decline of growth and proliferation, suggesting a possible role of proto-oncogenes for this protein.

PATZ1 expression and function in thyroid cancer [27] was analyzed, identifying a potential oncosoppressorrole, mainly involved in the inhibition of epithelium-mesenchyma transition and in cell migration. In fact, the immunohistochemical expression is reduced in tumor tissue compared to normal, with differences in intensity: slightly higher in well-differentiated cancers, reduced or even absent in poorly differentiated and anaplastic forms. It was observed, in poorly differentiated and anaplastic forms, a particular trend of the protein to delocalize from the nucleus to the cytoplasm. These observations could lead to thinking at the loss of PATZ1 and its

cytoplasmic location as a possible indicator of an undifferentiated, mesenchymal, and more aggressive phenotype.

In thyroid cancer, PATZ1 expression seems to start up p53 pathway that is implicated in the blockade of epithelium-mesenchymal transition through the down regulation of some genes (such as EpCAM, a stabilizing molecule inhibitor intercellular junctions , such as E-caderine, or through the direct inhibition of adhesion membrane components such as fibronectin) or the up regulation of actinic dynamics (RhoE and NOTCH). This effect is also observed when p53 gene is mutated.

From these evidence, it is apparent that PATZ1 is a protein whose role in cancer is not well-defined: it may play both as oncoppressor and as oncogene. The reason why this protein has great versatility is unknown, as well as its mechanism of action.

As with all members of the POK protein family, transcriptional activity is dependent on the formation of oligomers, mediated by the POZ domain, conferring a role of architectural transcription factor, rather than typical transcriptional actor, acting as repressor or activator, depending on the partner. In fact, for PATZ1 it has been observed a role of activator or repressor of c-myc, of activator of mast cell protease 6 and of FGF4, and of repressor of androgen receptor gene, CD8 and BCL6.

PATZ1 gene maps to chromosome 22 where is also the fragile site of FRA22B, affected by heterozygosity loss, that is typical of several solid tumors, thus supporting an onco suppressor role for this protein. Moreover, both homozygous and heterozygous knockout mice may spontaneously develop several tumors, such as non-Hodgkin BCL6 (+) lymphomas, sarcomas, and hepatocellular carcinomas. On the other hand, in some malignant neoplasms (colon, testicle and breast) an over-expression of PATZ1 has been observed, as it was seen that a down-regulation of the gene may block colon cancer growth and increase the sensitivity of gliomas to apoptotic stimuli.

2.3 Role in stemness

In normal tissues, cells are organized hierarchically. At the apex of the pyramid there is a stem cell that originates two “daughter cells”, a stem cell and a cell that will start a differentiation program; that cellular division is therefore defined asymmetric (127). Cells that lost their staminality status are defined as progenitor cells (or also transit-amplifying cells) and, present in many normal tissues, they represent intermediate forms between stem cells and their fully differentiated descending cells that have terminated their cycles growth and division (128). Consequently, progenitor cells can produce dozens, if not hundreds of progeny that are

differentiated from a single division of the original stem cell; stem cells may therefore rarely replicate, even in tissues that have a continuous cell replacement (intestinal mucosa, for example).

The same replicative pattern [28] also applies to tumor tissues, whose progenitor is the CancerStem Cell (CSC) cell, capable of self-regenerating and of producing numerous neoplastic progenitor cells that constitute the tumor. Although stem cell and progenitor cell are genetically identical, the latter, having lost its ability to self-regenerate, it has lost the ability to regenerate the tumor. Tumor stem cell shares the same environmentwith the normal counterpart, continuously fed by the presence of autocrine signals [29].

Although tumor stem cells represent the minority of the cellular population that makes up a tumor, they are responsible for tumor conservation and progression as well as the ability of the tumor to reproduce in xenograft murine models. Murine experiments have shown that depletion of tumor stem cells makes difficult to generate the tumor in xenograft transplantation and prolongs the survival of tumor carriers [30-32]. While the feasibility of using tumor brain stem cells as potential therapeutic targets in glioblastomas has recently been validated in vivo (134), the biological mechanism that is at the basis of their functioning is unknown.

The relationship between PATZ1 and staminality is subject to continuous research stimulated by various evidences. Recently, PATZ1 [33] has been shown to act as a pluripotency regulator in embryonic stem cells (ESCs), directly implicated in the control of pluripotency master gene, such as Pou5f1 and Nanog which, together with Sox2, are needed for self-immune and pluripotency of ESCs.

Embryonic stem cells are obtained from in vitro culture of cells extracted from the blastocyst's inner cell mass (IMC, Inner Cell Mass), in the pre-implantation phase [34,35]. These are cells characterized by two fundamental properties, the ability ofself-keeping, or to stay in a proliferative state for a long time, and of pluripotency, or the ability to differentiate into different types of specialized cells. ESCs may self-generate, by the action, in the culture medium, of leukemia inhibitor factor (LIF, belonging to the cytokine family of IL6 and acting through the activation of the Stat3 gene) and bone morphogenetic protein 4 (Bmp4) in the rat [36,37], and the basal fibroblast growth factor (bFGF) and the transforming growth factor β (TGFβ) in humans [38,39]. Although there are differences between murine form and human form of ESCs, the factors (Oct4, Sox2, Klf4 and c-Myc) that are responsible for maintaining a state of indifferentation of embryonic stem cells are the same in humans and in mouse.Pluripotency factors, known as the Yamanaka factors [40], have many target genes (thousands of orders) and are implicated in numerous pathways (development, metabolism, cancer, etc). Oct4, Sox2 and

Klf4 can also self-regulate, unlike c-myc. Their mechanism of action is not clear and often the interconnection between the different pathways may occur.

Oct4 (Octamer binding transcription factor 4, binding nucleotide octamer ATTTGCAT), also known as POU5f1 (POU domain, class 5, transcription factor 1) is present in embryonic tissues at different concentrations: high in the hypoblast, intermediate in the internal cell mass and low in the trophoectoderm. Demethylation of DNA is essential for its transcription. Oct4 forms a trimeric complex with Sox2 and is highly expressed in the developing brain, locating mainly in specific cellular layers of the cortex, hippocampus, olfactory bulbs, and cerebellum.

Sox2 (SRY, SexdeterminingRegion Y-box2) is an essential transcription factor in the self-maintenance of embryonic and neural stem cells. In neurogenesis, Sox2 is expressed developmental cells of the neural tube, as well as in proliferating progenitors of the central nervous system. It is down-regulated at the end of the cell cycle of progenitor cells, when these become post-mitotic cells. Cells expressing Sox2 are both self-regenerating and differentiating neuronal cells. Sox2, along with Oct4, binds Nanog promoter, regulating the expression of downstream genes implicated in self-maintaining ESCs.

KLf4 (Kruppel-likefactor) is a factor that belongs to the family of proteins with "zinc finger" domain, whose peculiarity is the presence, at the C-terminal end, of 2 highly conserved C2H2 domains, containing a zinc finger pattern. It is a fast response mediator to signals triggered by LIF-Stat3 and directly links Nanog's promoter to help Oct4 and Sox2 to regulate Nanog's expression**.**

c-Myc, carries out numerous cellular functions and is involved in many biological pathways, including the control of self-regeneration in embryonic stem cells. Mapping the target genes of these factors suggested that its role in maintaining pluripotency of ESCs should be different from the so-called "core" factors (Nanog, Sox2, and Oct4). c-Myc has many more target genes than other "core" factors and it is mostly involved in pathways associated with metabolism and protein synthesis, rather than in pathways related to development.

By gene expression analysis in cells of the Inner Cell Mass in the blastocists of the mouse, it has been observed that PATZ1 is much more expressed than in non-pluripotent trophoectoderm[41], as well as in Oct4 + cells compared to Oct4- [42]. Furthermore, the genomic region of PATZ1 represents the binding site of important factors (Oct4, Sox2, Nanog, Klf4 and c-Myc) [43,44]. PATZ1, in turn, is able to control the expression level of pluripotency genes, such as Nanog and Pou5F1, and its knockdown is able to determine, in murine models, the differentiation of ESC cells [45]: we have seen , in fact, by PATZ1 shutdown, that there is an

increase in the expression of markers of the trophoectoderm, endoderm and mesoderm and a reduced expression of pluripotency genes (confirmed by immunoblot techniques and gene expression analysis in microarrays). It has been identified in the CR4 region, the exact binding site of PATZ1 on the promoter of the Pou5f1 gene, which is in turn bound to other factors (148, 149, 150) such as Nanog and Oct4; it is also known that PATZ1 binds the proximal promoter of Nanog gene. Gene mapping techniques have highlighted the binding sites of PATZ1 factor in numerous genes, which in turn have been subjected to genetic ontology studies from which it is apparent that these genes are involved mainly in embryonic development but also in cellular proliferation, metabolism, and apoptosis. Many of PATZ1 binding sites are often shared with pluripotency transcription factors, though not belonging to the core of pluripotency factors or the c-Myc family. The important role of PATZ1 in regulating mouse embryonic stem cells has not yet been proven in human counterparts, but being the transcriptional network similar in the two species, it is very likely that it will be demonstrated.Undoubtedly, it is of great interest that, at the final stage of the development of mouse embryos, the expression of PATZ1 protein is confined to districts that host proliferating neural stem cells [46].

Studies on the testicle [47,48] demonstrated that POK protein family Plzf, regulates the mechanism required for the self-regeneration of spermatogenesis stem cells, interacting with Oct4 transcription factor; moreover, all the morphological alterations observed in the testes of Plzf-null mice are the same as those observed in PATZ1-null mice, demonstrating that PATZ1 probably also plays a role in testicular stenitis.Recently, it has been shown that pluripotent state can be generated by somatic mouse cells through the ectopic expression of Yamanaka transcription factors [40] (Oct4, Sox2, Klf4 and c-Myc). Induced pluripotent stem cells (iPSCs) resemble embryonic stem cells, also having the ability to self-sustain pluripotency and differentiate into many cell types. The exact mechanism of induction of pluripotency has not been well understood, but it undoubtedly represents a great possibility with extensive potentials for application in regenerative medicine. There are "barriers" that the somatic cell needs to overcome in order to be reprogrammed in a pluripotent stem cell. The reprogramming process is a dynamic process that involves a cascade of cellular events such as gene mutations responsible for differentiation along a specific line, pluripotency gene re-activation, mesenchyma-epithelial transition (MET), cellular senescence overcoming , acquisition of cellular immortality, re-activation of chromosome X and reset of chromatin signature.Cell senescence appears to be a limiting factor for reprogramming at the initial stage. The locus of the oncosoppressor Ink4a / Arf plays a critical role in regulating senescence in many types of cells. For example, silencing Ink4a / Arf locus or the ablation of its activator Jmjd3 seems to reduce cellular senescence and significantly improve the efficiency of reprogramming.

The change of the epigenetic panorama represents another barrier mechanism for reprogramming. Pluripotent cells possess a highly plastic chromatin structure because they are globally open and decondensed with a high ratio between the active and the repressed form. In order to successfully complete the reprogramming process of somatic cells in which chromatin is predominantly condensed, it is necessary to make possible the conversion into open form, thus accessible to the action of the transcription factors. In fact, inhibition of chromatin condensation, ablation of the NuRD / Mbd3 repression complex, inhibition of HDAC or H3K4me3 activity strongly increases the induction of iPSCs [49]. The mechanism by which epigenetic factors have an impact in the reprogramming process is not well known.

In this regard, we have investigated the role of PATZ1, as this is a transcription factor that operates differently, depending on the cellular context and being implicated in maintaining the pluripotency status in ESCs.

It has been seen that PATZ1 hyper-expression inhibits the reprogramming process mediated by OKSM, probably through the control of c-Myc transcription, cell senescence and chromatinic regulation [50]. This effect is also obtained if the expression of PATZ1 is induced during the reprogramming, not at the beginning. Partial depletion (heterozygotesKnockout), however, promotes the genesis of iPSCs by the downregulation of repressive histones and the up-regulation of active histones, leading to the creation of a more open and accessible chromatin. Moreover, it has been seen that PATZ1+/- manages to pass the Ink4a/Arflocus, a locus of senescence. The total loss of PATZ1 (PATZ1-/-) finally leads to cellular senescence and therefore the blockage of cellular reprogramming.During cell reprogramming, PATZ1 acts by blocking the expression of c-Myc which, in turn, counteract the inhibitory action of PATZ1 and it appears that, when over-expressed, the protein with the "Zn finger" domain would cause an over-expression of p16, a senescence marker, and p53. Gene expression studies on murine embryo fibroblasts at various levels of expression of PATZ1 (+/+, +/- and -/-) have shown that a number of genes are up-regulated, while others are down-regulated; with the study of Genica Ontology it has been seen that these are transcription factors, many of which are related to development, cellular differentiation, but also to neurophysiology, factors implicated in the induction of mesenchima-epithelium transition or chromatinic regulation (histones deacetylaseHdac 2,4,11 are down-regulated with PATZ1 shutdown, while acetylases Hat1 and Kat2a are up-regulated).The mechanism by which the heterozygous form (+ ;-) could overcome the obstacle represented by senescence is mediated by histone acetylation which promotes an open chromatin state accessible to the activation of the transcriptional network of pluripotency. In fact, in the Ink4a locus (gene implicated in senescence), the inactive H3K27me3 histamine (so called because of lysine 27 tri-methylate) is down-regulated.

From these observations it is concluded that PATZ1 has an effect that is dependent not only by the context, but also by the concentration.

AIMS AND SCOPES

The aim of the present work was to characterize the immunohistochemicalexpression of PATZ1 protein in gliomas, compare it with the normal brain and evaluate its possible prognostic role. Furthermore, we studied its co-localization with stem cell markers by the help of immunofluorescence and cell cultures. And finally, we assessed the eventual correlation of PATZ1 with the G-protein coupled receptor CXCR4.

METHODS

1. Tissue specimens

45 patients diagnosed with glioblastoma and 22 with oligodendroglioma were included in the study. They had all undergone a complete excision of the tumor at first surgery. All the cases were identified between 2004 and 2013 and the diagnoses were made in accordance with the 2007 WHO classification [5]. This time interval was chosen in order to ensure a clinical follow-up period of at least 2 years for each identified case. All the cases were reviewed to evaluate adequate representative formalin-fixed paraffin-embedded tissue in order to perform immunohistochemical assay. We excluded those cases for which data of outcome were unavailable and for which diagnostic tissue was insufficient. Informed consent for the scientific use of biological material was obtained from all patients and the work has been approved by the local Ethical Committee (CEI 203/15 of 12/11/2015).

2. Immunohistochemical analysis

4 μm sections were used for immunohistochemistry. Sections were dewaxed in xylene, hydrated in graded series of alcohol and subjected to heat-induced antigen retrieval. After blocking endogenous peroxidase activity, the tissue was incubated with antibody anti- PATZ1 (polyclonal rabbit, R1P1 [51]; 1: 500 dilution, overnight incubation). Subsequently, the slices were rinsed and incubated with the biotinylated secondary 15

antibody, at room temperature, for 30 minutes. The bound antibody complexes were stained for 3-5 minutes or until appropriate for microscopic examination with diaminobenzidine, and slides were then counterstained with hematoxylin (30s) and mounted. All slices were reviewed by two experienced pathologists (M.L.D., E.G.).

The assessment of PATZ1 (nuclear) staining was based on the percentage of positive cells: no signal was set as “0”, ≤10% as “+”, >10% and <50% as “++” and ≥50% as “+++”. We defined high expression of PATZ1 as >10% of cells staining positive, and low expression as ≤10% of cells staining positive.

3. Immunofluorescence and confocal microscopy

For multiple-labeling immunofluorescence, tissues slides were dewaxed, hydrated and antigen retrieval was performed using Dewax and HIER Buffer L (Thermo Fisher Scientific, Cheshire, UK) as previously described [52]. They were incubated with the mixture of two primary antibodies anti-NESTIN (mouse monoclonal, sc23927, Santa Cruz Biotechnology, Santa Cruz, CA; 1:200 dilution, 90 minutes incubation) and anti-PATZ1 (rabbit polyclonal, R1P1; 1: 500 dilution, overnight incubation) or anti PATZ1 and anti-OCT-3/4 (mouse monoclonal, sc-5279 Santa Cruz Biotechnology; 1:100 dilution, 90 minutes incubation) in 1% BSA in PBS-T in a humified chamber overnight at 4°C. Fluorescent secondary antibodies, raised against different species (Alexa Fluor 594, with red signal, against rabbit and Alexa Fluor 488, with green signal, against mouse), were used to locate the antigen/primary antibody complexes. Counter staining was made with Hoechst 33258 (nuclear blue staining) present in mounting medium (PBS:Glycerol = 1:1). Experiments were carried out on an inverted and motorized microscope (Axio Observer Z.1) equipped with a 63x/1.4 Plan-Apochromat objective. The attached laser scanning unit (LSM 700 4x pigtailed laser 405-639, Zeiss, Jena, Germany) enabled confocal imaging. For excitation, 405 nm, 488 nm and 555 nm lasers were used. Fluorescence emission was revealed by MBS 405/488/555/639 for Hoechst 33258, Alexa Fluor 488 and Alexa Fluor 594. Triple staining immunoflourescence images were acquired separately in the blue, green and red channels at a resolution of 1024x1024 pixels, with the confocal pinhole set to one Airy unit and then saved in TIFF format.

To assess the stemness of GSCs, NANOG (rabbit polyclonal, ab80892 Abcam; 1:200 dilution), SOX-2 (mouse polyclonal, AB5603 Millipore; 1:500 dilution), OCT-4 (rabbit polyclonal, sc-5279 Santa Cruz; 1:250 dilution) and NESTIN (mouse monoclonal, 92590 Chemicon; 1:100 dilution) expression was evaluated. PATZ1 (rabbit polyclonal, R1P1, 1:500 dilution) expression was analyzed as well. Briefly, cells were fixed in 4% paraformaldehyde for 20 minutes at room temperature (RT) and permeabilized for 10 minutes at RT with 0.1% Triton X-100 (Sigma-Aldrich) before exposing them to primary antibodies, that were incubated over-night at 4°C. Subsequently, Alexa Fluor 488 and Alexa Fluor 555 dyes labeled secondary antibodies against mouse and rabbit, respectively, diluted 1:800 in PBS, were employed for 1 hour in a humidified chamber at

37°C (Molecular Probe, Invitrogen). Lastly, slides were mounted using Vectashield (Vector), as mounting medium, added with 0.1 μg/ml DAPI (Sigma) for nuclear staining. Images were acquired utilizing a live cell imaging dedicated system consisting of a Leica DMI 6000B microscope connected to a Leica DFC350FX camera (Leica Microsystems, Wetzlar, Germany) and equipped with a 63X/1.4 oil immersion objective or a 40X/1.25 oil immersion objective. Adobe Photoshop software was utilized to compose and overlay the images and to adjust contrast.

4. Cell cultures and transfection

The independent ethic committee of the AziendaOspedaliero-Universitaria of Udine has approved the research (Consents 102/2011/Sper and 196/2014/Em). Informed written consents were obtained from patients and all clinical investigations have been conducted according to the principles expressed in the Declaration of Helsinki.

GSCs (n=11) were isolated as previously described [53,54]. Briefly, human GBM samples were mechanically-enzymatically dissociated and cells less than 40μm in diameter cultured on laminin-coated dishes in a growing medium composed as follows: Neurobasal-A medium (Gibco by Invitrogen, Carlsbad, CA), 2mM L-glutamine (Sigma-Aldrich, St. Louis, MO,), 1X N2 supplement (Gibco by Invitrogen), 25mg/ml Insulin, Penicillin-streptomycin, 100mg/ml human apo-trasferrin (Sigma- Aldrich), 1X B-27 supplement (Gibco by Invitrogen), 20 ng/ml recombinant human basic fibroblast growth factor (h-FGF-basic) (Peprotech, Rocky Hill, NJ), 20 ng/ ml human epidermal growth factor (h-EGF) (Peprotech). Then cells were cultured in an incubator at 37°C, 5%O2/5%CO2 and analyzed at the third passage in culture. From six GBM samples we isolated, in addition to GSCs, the matched non-stem tumor cells by growing dissociated cells in DMEM (Gibco by Invitrogen) supplemented with 10% fetal bovine serum (FBS) (EuroClone, Pero, Italy) and 100 U/ml Penicillin 100 μg/ml Streptomycin. Cells were grown in an incubator at 37°C, 5%O2/5% CO2 and analyzed at the first passage in culture.

Human GBM U87MG (American Type Culture Collection, ATCC no. HTB-14), were grown in Dulbecco's modified Eagle medium (DMEM) supplemented with 10% FBS. To obtain tumorspheres, U87MG cells were grown at low density (2000 cells/ml) in Stem cell medium (SM) [DMEM-F12 supplemented with 1% B27 (Sigma-Aldrich), 10 ng/ml h-FGF

(Sigma-Aldrich) and 20 ng/ml h-EGF (Sigma-Aldrich)] for 12 days. U87MG tumorspheres were induced to differentiate through the addiction of 10% FBS in SM medium. The cancer stem cell phenotype of these

cells was confirmed by assessing the expression of the stemness markers PDGFRß, NANOG and SOX-2.

VS-GB primary cell culture was derived from GBM specimens and grown as described previously [55]. They were transiently transfected by JetPRIME (Polyplus transfections, Illkirch, France) with 10 μg of HA-PATZ1 plasmid encoding for PATZ1 variant 4 or 10 μg of the empty vector pCEFL-HA as negative control, according to manufacturer's instruction.

5. RNA extraction and quantitative real time (qRT)-PCR

Total RNA from cells was purified by TRIzol (Invitrogen). After digestion of the residual genomic DNA by DNase I (Qiagen, Milano, Italy), RNA was reverse transcribed by SuperScript III cDNA synthesis kit (Invitrogen). cDNA was used to perform qPCR reactions with SYBR Green Master Mix gene expression kit (Biorad, Segrate, Italy) in 96-well plates with a LightCycler 480 system (Roche, Monza, Italy). The PCR conditions were as follow: 95°C for 3 minutes; 45 cycles at 95°C for 10 seconds, 60°C for 20 seconds and 72°C for 60 seconds. Primer pairs used (300 nm each) were as follows: *PATZ1* (5'-TACATCTGCCAGAGCTGTGG- 3'/5'-TGCACCTGCTTGATATGTCC-3'); *GAPDH* (5'-GTCTCCTCTGACTTCAACAGCG-3'/5'-ACCACCCTG TTGCTGTAGCCAA-3'). *CXCR4* (5'-TGAGAAG CATGACGGACAAG-3'/5'-AGGGAAGCGTGATGAC AAAG-3'); *β-ACTIN* (5'-CAAGAGATGGCCAC GGCTGCT-3'/5'-TCCTTCTGCATCCTGTCGGCA-3'). Gene expression changes were calculated using the 2(-Delta Delta C(T)) method [56].

6. Protein extraction and western blot analysis

Cells were lysed in buffer containing 1% Nonidet P-40, 1 mmol/liter EDTA, 50 mmol/liter Tris-HCl (pH 7.5), and 150 mmol/liter NaCl supplemented with Complete protease inhibitors (Roche). Total proteins were resolved in a 10-12% polyacrylamide gel under denaturing conditions and transferred to nitrocellulose filters for Western blot analyses. Membranes were blocked with 5% BSA in TBS and incubated with the primary

antibodies. Membranes were then incubated with the horseradish peroxidase–conjugated secondary antibody (1:3.000) and the reaction was detected with a Western blotting detection system (enhanced chemiluminescence; GE Healthcare). The primary antibodies used were: anti-PATZ1 [51]; anti-NESTIN (sc- 23927, Santa Cruz Biotechnology, Santa Cruz, CA); anti- PDGFRβ (3169, Cell Signaling Technology, Boston, MA); anti-NANOG (sc-134218, Santa Cruz Biotechnology); anti- SOX2 (sc-20088, Santa Cruz Biotechnology); anti-CXCR4 (C8727, Sigma-Aldrich). To ascertain that equal amounts of protein were loaded, the membranes were incubated with anti-ACTIN (sc-1616-R, Santa Cruz Biotechnology) or anti-VINCULIN (sc-7649, Santa Cruz Biotechnology) antibodies.

7. Data mining

For PATZ1 mRNA expression analysis and correlation with clinical, molecular and cell phenotype, the Genomics Analysis and Visualization platform (http://r2.amc.nl) was used with the following datasets: 1) GSE9385 [57], including 6 adult non diseased brain, 26 glioblastomas and 21 oligodendrogliomas,; 2) GSE8049 [58], including 9 different glioblastoma-derived neurosphere cultures in two biological replicates; 3) GSE15209 [59], including stem cells derived from 7 GBMs, 2 oligoastrocytomas, 5 normal fetuses and primary biopsies from 6 normal brains; 4) GSE18015 [60], including 8 gliomas sorted for CD133 expression; 5) the TCGA dataset Tumor Glioblastoma - 540 - MAS5.0 - u133a (n = 540) (http://cancergenome.nih. gov), including 85 samples sub-classified in classical (n = 17), mesenchymal (n = 27), neural (n = 17) and proneural (n = 24) GBM [7], to correlate *PATZ1* expression to GBM subtype and specific gene signatures. The last dataset was also used for Overall and Progression-free survival analysis using the scan cut-off mode based on median PATZ1 expression and specifying the proneural track subset.

8. Statistical analysis and Kaplan-Meier survival curves

The Fisher's exact test was used to evaluate the correlations between PATZ1 score and the clinical variables (age, gender, site, oligodendroglioma grading).

All correlations within the TCGA and other public datasets were assessed by Pearson's $\chi 2$ test or one-way analysis of variance (ANOVA), through the R2 platform (http://r2.amc.nl).

Kaplan-Meier survival curves were used to analyze OS and PFS, and statistical significance was assessed by the log-rank test. In Figure 6A, the stratification of High/Low PATZ1 was based on the percentage of cells expressing nuclear PATZ1 protein by immunohistochemistry (High: > 50%; Low: < 50%). The stratification of High/Low *PATZ1* and High/Low *CXCR4* in the TCGA dataset was based on RNA expression using a cutoff of 100.6 and 197.7, according to the scan function of the R2 platform used, where an optimum survival cutoff is established based on statistical testing (log-rank test).

PATZ1 expression on human derived stem cells was expressed as mean ± standard deviation. Comparisons between two groups were performed by paired or unpaired t test, as appropriate.

All statistical analyses were performed using GraphPad Prism 5 software (GraphPad Software, La Jolla, CA). A probability (p) value less than 0.05 was considered statistically significant.

RESULTS

1. PATZ1 is expressed in human gliomas and is enriched in the proneural subtype

Using paraffin embedded sections generated from surgical specimens collected at the Department of Advanced Biomedical Sciences, Pathology Section, of the University of Naples Federico II, we analysed by immunohistochemistry PATZ1 expression in 45 grade IV GBM, 22 oligodendrogliomas (10 grade III and 12 grade II) and 26 perilesional normal brain parenchymas. Of 45 GBM patients included in the study, 30 were males and 15 females, aged between 26 and 81 years. The lesion was mainly localized in the temporal lobe in 22 cases, parietal in 11 cases, frontal in 9 cases, occipital in 2 cases and 1 in the corpus callosum (Supplementary Table 1). Of 22 oligodendroglioma patients 15 were males and 7 females, aging from 22 to 69 years. 14 cases were frontal, 4 temporal, 3 occipital and 1 was an intramedullary metastasis (Supplementary Table 2).

We have observed that PATZ1 protein is expressed in neurons (mainly in the nucleus) but not in glial cells of all perilesional normal brain tissues (Figure 5A), whereas it is expressed in a high percentage of GBM (69%) with a mainnuclear, but sometimes cytoplasmic localization (Figure 5B, Supplementary Table 1) and oligodendrogliomas (54%) (Supplementary Table 2).

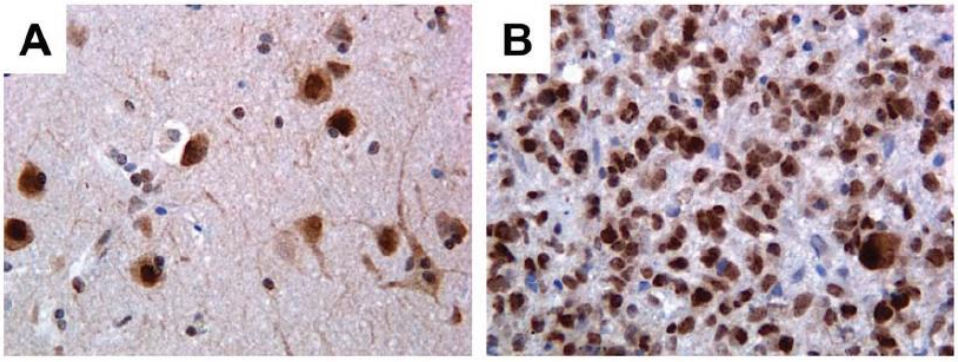

Figure 5: Immunohistochemicaldetection of PATZ1 in human GBM and perilesional normal cortex. (A) Perilesional normal cortex: only neurons stain positively, mainly in the nucleus, while glial cells are negative. (B) Representative GBM: most of neoplastic cells are positive. Original magnification: 40x

Among positive samples, PATZ1 immunoreactivity was variable in both GBM and oligodendrogliomas, including samples scored + (≤10%), ++ (>10% <50%), +++ (≥ 50%). Of 31 GBM positive for PATZ1 staining, 17 displayed +, 9 ++ and 5 +++ score (Figure 6A–D, Supplementary Table 1). Among the 12 oligodendrogliomas expressing PATZ1, 4 cases had +, 5 ++ and 3 +++ score (Figure 6E–6H, Supplementary Table 2). Among the assessed clinicopathological features of GBM (age, gender, site), a high significant correlation and a trend

to be correlated with PATZ1 expression was present in the male gender (p = 0.0028) and younger patients (p = 0.0695), respectively. Moreover, a statistically significant correlation was observed between PATZ1 immunoreactivity and grading (p = 0.0286) in oligodendrogliomas (Table 1).

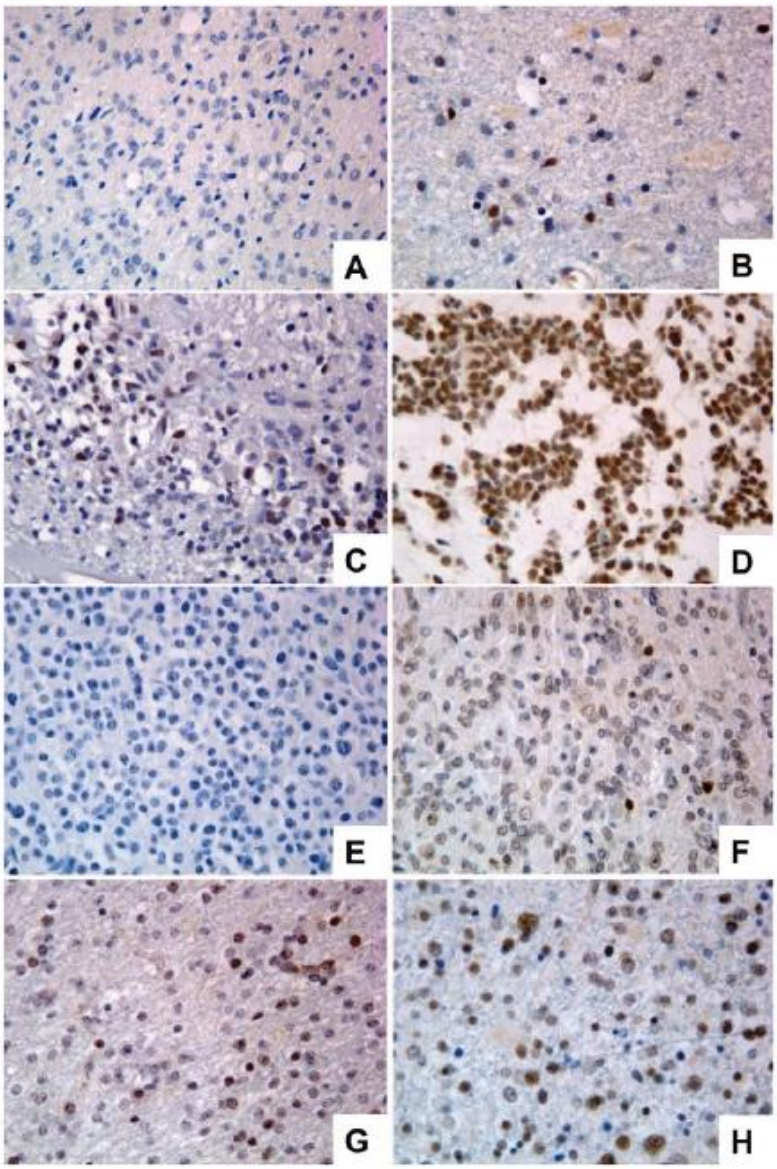

Figure 6: Immunoreactivity score in GBM and oligodendrogliomas stained for PATZ1. (A) Representative GBM scored 0.**(B)** Representative GBM scored +. **(C)**Representative GBM scored ++. **(D)**Representative GBM scored +++. (E)Representativeoligodendrogliomascored 0.**(F)**Representativeoligodendrogliomascored +. **(G)**Representativeoligodendrogliomascored ++. **(H)**Representativeoligodendrogliomascored +++. Originalmagnification: 40x

Table 1: Fisher's exact test: clinicopathological features and PATZ1 expression

Variables		PATZ1 expression		
GBM	**n.**	+/++/+++	-	**p**
Age	45			
<60	11	10 (91%)	1 (9%)	0.0695
≥60	34	21 (62%)	13 (38%)	
Gender	45			
Males	30	27 (90%)	3 (10%)	**0.0028**
Females	15	7 (47%)	8 (53%)	
Site	42			
Temporal	22	14 (64%)	8 (36%)	0.5586
Parietal	11	9 (82%)	2 (18%)	
Frontal	9	6 (67%)	3 (33%)	
Oligodendrogliomas				
Age	22			
<60	17	9 (53%)	8 (47%)	0.7805
≥60	5	3 (60%)	2 (40%)	
Gender	22			
Males	15	9 (60%)	6 (40%)	0.4520
Females	7	3 (43%)	4 (57%)	
Site	21			
Frontal	14	6 (43%)	8 (57%)	0.1974
Temporal	4	2 (50%)	2 (50%)	
Occipital	3	3 (100%)	0 (0%)	
Grading	22			
II	12	4 (33%)	8 (67%)	**0.0286**
III	10	8 (80%)	2 (20%)	

By analysing public datasets through the R2: genomic Analysis and Visualization platform (http:// r2.amc.nl), we confirmed in an independent sample cohort of 6 adult non diseased brains, 26 GBMs and 21 oligodendrogliomas [57] that *PATZ1* is significantly more expressed in gliomas (including GBMs and oligodendrogliomas) compared to non diseased brain samples (Figure 7A). Moreover, in a data set from the Tumor Cancer Genomic Atlas (TCGA), including 85 samples, sub-classified in classical (n = 17), mesenchymal (n = 27), neural (n = 17) and proneural (n = 24) GBM, we found that *PATZ1* expression specifically correlates with the molecular subtype, being highest in proneural and lowest in mesenchymal subtype, with significant differences between each subtype (Figure 7B). Consistently, by studying the gene signature correlated with the expression of *PATZ1* in the context of GBM, we found that PATZ1 expression positively associates with proneural genes, including *SOX2*, *OLIG2*, *DLL3*,*NOTCH1*, *PDGFRα*and many others, while negatively associates with the mesenchymal marker CD44 and many other genes characterizing the mesenchymal signature (Table 2 and Supplementary Table 3).

Taken together protein and gene expression data, PATZ1 is overexpressed in gliomas compared to normal glia and appears as a specific biomarker of the proneural GBM sub-type.

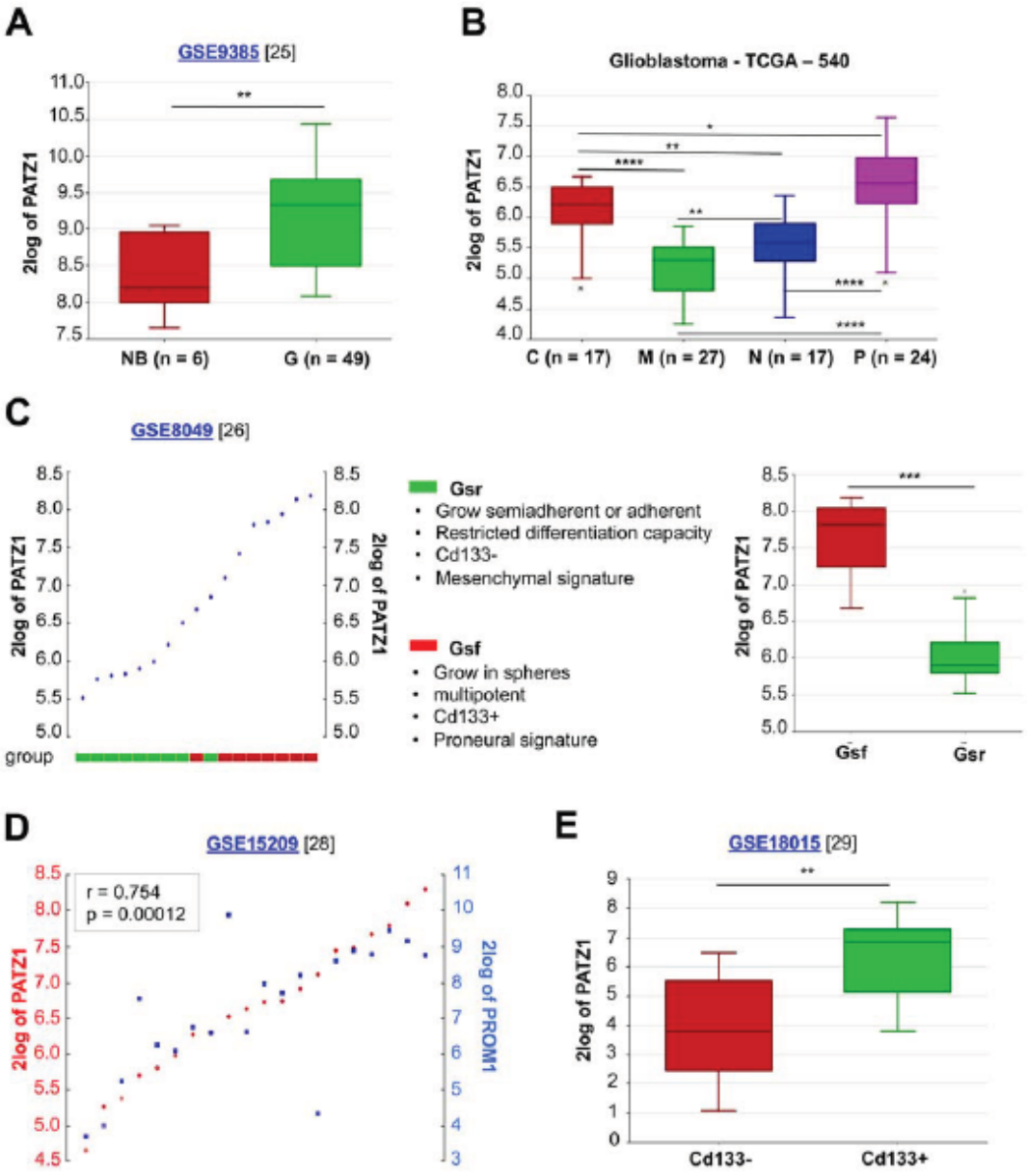

Figure 7: In silico meta-analysis of PATZ1 expression in human GBM tissues and cell lines. (A) Box-plot comparing PATZ1 expression in normal brain (NB) and gliomas of different grade (G). The data were analyzed by one-way analysis of variance (ANOVA) through the R2 web platform**(B)** Box-plot showing PATZ1 expression in the different GBM subtypes and statistical analysis of the differences among them. C= Classical, M= Mesenchymal, N= Neural, P=Proneural. The data were analyzed by one-way analysis of variance (ANOVA) through the R2 web platform. (C)On the left, YY-plot in GSCs (ordered by PATZ1 expression). The cells are divided in two groups as indicated in the figure. On the right, box-plot comparing PATZ1 expression in the two groups. **(D)** YY-plot correlating PATZ1 and PROM1 expression in stem cell derived from GBM (n=7), oligoastrocytoma (n=2), normal human foetus (n=5) and primary biopses of non-malignantbrain tissue (n=6). Significance of correlation (inbox) was analyzed by Pearson's χ^2 test through the R2 web platform (http://r2.amc.nl). **(E)** Box-plot comparing PATZ1 expression in primary GBM sorted for CD133 expression (negative/positive). The data were analyzed by one-way analysis of variance (ANOVA) through the R2 web platform. *, $p<0.05$; **, $p<0.01$; ***, $p<0.001$; ****, $p<0.0001$. Datasets for each cohort of samples are indicated in the figure with relative reference in brackets. 2log og PATZ1= logarithmic values of PATZ1 expression with base of 2

Table 2: Correlations between *PATZ1* and the proneural and mesenchymal signature in GBM[a]

Proneural signature			Mesenchymal signature		
Gene	**r[b]**	**p**	**gene**	**r**	**p**
CHD7	0.649	3.9e-62	*HEXB*	-0.597	3.8e-50
CSNK1E	0.633	3.1e-58	*SQRDL*	-0.583	2.7e-47
MARCKSL1	0.592	4.4e-49	*TMBIM1*	-0.537	4.1e-39
SOX4	0.580	7.1e-47	*IL15*	-0.535	7.1e-39
NOTCH1	0.574	1.0e-45	*RAB32*	-0.528	1.0e-37
MAP2	0.564	9.4e-44	*ANXA4*	-0.524	5.1e-37
SOX11	0.557	1.1e-42	*S100A4*	-0.523	5.7e-37
DLL3	0.549	3.8e-41	*FCGR2B*	-0.522	1.0e-36
PODXL2	0.545	1.3e-40	*RRAS*	-0.518	4.4e-36
MMP16	0.539	1.4e-39	*P4HA2*	-0.513	2.2e-35
FXYD6	0.535	6.9e-39	*VAMP5*	-0.505	3.8e-34
TOP2B	0.532	1.8e-38	*NPC2*	-0.499	2.7e-33
PHF16	0.532	2.2e-38	*CAST*	-0.497	6.3e-33
SEZ6L	0.526	2.1e-37	*PLS3*	-0.497	4.7e-33
BCAN	0.524	4.0e-37	*COPZ2*	-0.495	1.1e-32
CRMP1	0.519	3.1e-36	*PLAUR*	-0.495	9.4e-33
NLGN3	0.518	4.2e-36	*CLEC2B*	-0.490	5.4e-32
WDR6	0.511	3.9e-35	*LGALS3*	-0.477	3.9e-30
PHLPP1	0.500	1.8e-33	*LY96*	-0.476	5.6e-30
MTSS1	0.494	1.5e-32	*CLIC1*	-0.475	6.1e-30
OLIG2	0.494	1.6e-32	*PIGP*	-0.473	1.1e-29
NRXN2	0.488	1.2e-31	*ALOX5*	-0.466	1.0e-28
PAFAH1B3	0.488	1.2e-31	*TNFAIP8*	-0.465	1.3e-28
DBN1	0.484	4.1e-31	*CSTA*	-0.461	4.3e-28
MMP15	0.483	5.8e-31	*S100A11*	-0.461	5.0e-28
FLRT1	0.479	1.8e-30	*CTSB*	-0.453	4.9e-27
DPF1	0.479	1.9e-30	*CASP4*	-0.453	4.5e-27
ASCL1	0.479	1.7e-30	*ANXA2*	-0.447	2.9e-26
CRB1	0.476	5.3e-30	*RAB27A*	-0.442	1.1e-25
DCX	0.472	1.5e-29	*MGST2*	-0.440	1.9e-25
SATB1	0.472	1.6e-29	*SP100*	-0.439	2.7e-25
ZNF510	0.471	2.1e-29	*ARPC1B*	-0.437	4.6e-25
RUFY3	0.467	7.5e-29	*TLR2*	-0.437	4.4e-25
GNG4	0.467	7.8e-29	*ASL*	-0.433	1.6e-24
MYT1	0.461	5.1e-28	*KYNU*	-0.433	1.3e-24

(Continued)

Proneural signature			Mesenchymal signature		
Gene	r[b]	p	gene	r	p
CASK	0.451	9.9e-27	*PROCR*	-0.433	1.7e-24
CDK5R1	0.446	4.4e-26	*FHL2*	-0.433	1.4e-24
VAX2	0.442	1.1e-25	*LGALS1*	-0.432	2.1e-24
GSK3B	0.436	5.9e-25	*TIMP1*	-0.432	1.8e-24
NCAM1	0.430	3.7e-24	*PHF11*	-0.432	2.1e-24
MAPT	0.429	4.5e-24	*MAN1A1*	-0.425	1.3e-23
CKB	0.425	1.4e-23	*AMPD3*	-0.424	1.5e-23
CBX1	0.425	1.3e-23	*POLD4*	-0.418	7.2e-23
KIF21B	0.425	1.3e-23	*CYBRD1*	-0.418	7.1e-23
MYO10	0.424	1.6e-23	*CHI3L1*	-0.418	7.9e-23
NOL4	0.423	2.4e-23	*IFI30*	-0.416	1.2e-22
MPPED2	0.422	2.8e-23	*FCGR2A*	-0.414	2.1e-22
BCOR	0.420	5.4e-23	*ACSL1*	-0.413	3.0e-22
CSPG5	0.419	6.0e-23	*MAN2A1*	-0.413	2.7e-22
CLASP2	0.414	2.3e-22	*SYPL1*	-0.412	3.7e-22
HMGB3	0.406	1.5e-21	*IQGAP1*	-0.405	2.4e-21
TMCC1	0.403	3.3e-21	*RAC2*	-0.403	3.6e-21
NKX2-2	0.400	7.1e-21	*ICAM3*	-0.402	4.3e-21
RALGPS1	0.400	7.1e-21	*MS4A4A*	-0.401	6.6e-21
SOX2	0.399	9.7e-21	*CRYZ*	-0.401	6.2e-21
GRIA2	0.399	1.0e-20	*ANXA1*	-0.400	8.2e-21
TTYH1	0.397	1.4e-20	*PTGER4*	-0.396	2.1e-20
ZNF184	0.397	1.5e-20	*LTBP2*	-0.396	2.2e-20
SCN3A	0.396	1.9e-20	*SLC16A3*	-0.395	2.4e-20
KLRC3	0.394	3.2e-20	*NCF2*	-0.393	3.8e-20
AMOTL2	0.391	6.6e-20	*TGFBI*	-0.391	6.2e-20
TAF5	0.389	1.0e-19	*MAFB*	-0.390	7.6e-20
DUSP26	0.383	3.8e-19	*RHOG*	-0.388	1.4e-19
RAP2A	0.383	4.4e-19	*CTSC*	-0.387	1.5e-19
CDC7	0.380	8.1e-19	*SWAP70*	-0.386	2.2e-19
SRGAP3	0.377	1.7e-18	*IGFBP6*	-0.383	4.1e-19
WASF1	0.375	2.4e-18	*SERPINA1*	-0.382	5.3e-19
ICK	0.372	5.2e-18	*MFSD1*	-0.382	5.6e-19
RAD21	0.371	6.4e-18	*ACPP*	-0.381	6.1e-19
GSTA4	0.368	1.1e-17	*TNFAIP3*	-0.380	8.9e-19
SEC61A2	0.367	1.5e-17	*IL1R1*	-0.380	8.3e-19

(Continued)

Proneural signature			Mesenchymal signature		
Gene	r[b]	p	gene	r	p
EPHB1	0.364	2.8e-17	*SYNGR2*	-0.377	1.6e-18
DPYSL4	0.363	3.3e-17	*CASP8*	-0.376	1.9e-18
NRXN1	0.360	6.5e-17	*C5AR1*	-0.375	2.4e-18
PDGRA	0.352	3.6e-16	*CTSZ*	-0.375	2.6e-18
ERBB3	0.352	3.8e-16	*ARHGAP29*	-0.369	9.6e-18
ABAT	0.350	5.3e-16	*SHC1*	-0.366	1.8e-17
GADD45G	0.345	1.4e-15	*SERPINE1*	-0.366	1.7e-17
CDC25A	0.341	3.7e-15	*MSR1*	-0.366	1.9e-17
ATP1A3	0.338	5.8e-15	*FXYD5*	-0.365	2.2e-17
YPEL1	0.336	9.6e-15	*THBD*	-0.364	2.8e-17
FBXO21	0.335	1.1e-14	*LAIR1*	-0.363	3.6e-17
ARHGEF9	0.335	1.1e-14	*CD14*	-0.359	8.9e-17
HDAC2	0.331	2.2e-14	*GRN*	-0.358	1.1e-16
ZNF248	0.328	4.3e-14	*PTPRC*	-0.354	2.6e-16
FHOD3	0.324	8.5e-14	*LY75*	-0.353	3.1e-16
HOXD3	0.320	1.9e-13	*GNA15*	-0.350	5.6e-16
TSAPN3	0.318	2.8e-13	*VDR*	-0.349	7.1e-16
TOPBP1	0.318	3.0e-13	*CASP1*	-0.349	6.3e-16
EPB41L5	0.317	3.1e-13	*ITGB2*	-0.346	1.4e-15
BEX1	0.316	3.9e-13	*PTPN22*	-0.345	1.7e-15
DGKI	0.314	5.7e-13	*EMP3*	-0.345	1.7e-15
STMN1	0.314	6.1e-13	*TCIRG1*	-0.344	1.8e-15
CA10	0.308	1.7e-12	*SLAMF8*	-0.344	2.0e-15
MCM10	0.307	1.9e-12	*SIGLEC7*	-0.344	1.7e-15
P2RX7	0.305	3.0e-12	*ITGAM*	-0.338	5.7e-15
PDE10A	0.295	1.6e-11	*SCPEP1*	-0.336	8.8e-15
FGF9	0.293	2.2e-11	*TGFBR2*	-0.333	1.5e-14
RAB33A	0.293	2.1e-11	*STAT6*	-0.333	1.6e-14
TMEM35	0.290	3.6e-11	*LILRB2*	-0.332	2.1e-14
GRID2	0.290	3.6e-11	*SIGLEC9*	-0.330	3.0e-14
PPM1D	0.288	4.8e-11	*PLAU*	-0.324	8.6e-14
PAK7	0.286	6.6e-11	*ARSJ*	-0.324	9.5e-14
NANOG	0.284	1.0e-10	*SEC24D*	-0.323	1.1e-13
PPM1E	0.280	1.8e-10	*TRIM38*	-0.319	2.3e-13
MAST1	0.279	2.2e-10	*ELF4*	-0.318	2.7e-13

[a] All the genes belong to either the proneural or mesenchymal signatures as described by Verhaak et al. [7].

[b] Correlations were analyzed by Pearson's χ^2 test through the R2 platform (http://r2.amc.nl). For more correlations between *PATZ1* and the mesenchymal signature see ~~supplementary~~ Supplementary Table 5.

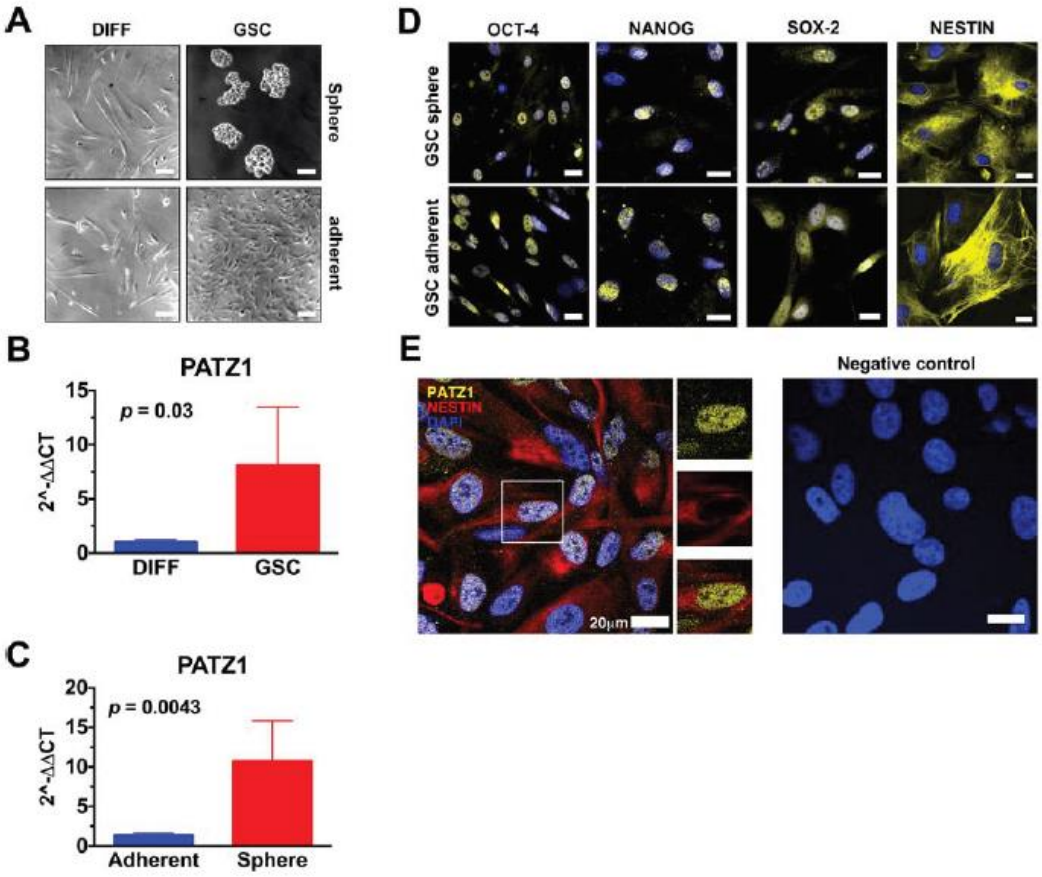

Fig.8: PATZ1 expression in GSC cultures. (A) Representative phase contrast pictures of human glioma cells cultured in media selective (GSC, right panels) or not (DIFF , left panels) for the growth of glioma stem cells. The upper-right panel displays GSC growing as neurosphere, while the lower-right panel displays GSCs growing in adhesion. Scale bar: 100 μm. **(B)** Gene expression changes of PATZ1 in human glioma cells grown in media selective (GSC) or not (DIFF) for the growth of GSC, as assessed by qRT-PCR. Data are presented as mean±SD. **(C)** Gene expression changesof PATZ1in GSC growing in adhesion (Adherent) or in suspension (Sphere), as assessed by qRT-PCR. Data are presented as mean±SD.**(D)** Representative immunofluorescence images depicting the expression of OCT4, NANOG, SOX-2 and NESTIN in GSC growing either in adhesion (GSC adherent, lower panels) or in suspensions (GSC shere, upper panels). Nuclei are depicted by the blue fluorescence of DAPI. Scale bar: 20 μm. (E) Representative confocal immunofluorescence image (merge image) showing the expression of PATZ1 (yellow fluorescence) and Nestin (red fluorescence) in GSCs. Nuceli are depicetd by the blue fluorescence of DAPI. Single immunodetection of either PATZ1 or Nestin in the inset areal, and digital merge of teh images, are shown in the middle. Negative control obtained by omitting the primary antibodies is shown on the right. Scale bar: 20 μm.

2. PATZ1 is preferentially expressed in glioma stem cells

It has been recently reported that a proneural-like gene expression signature is characteristic of GSCs characterized by a full stem phenotype (Gsf lines), growth as floating spheres, CD133 expression and multipotency, while a mesenchymal-like gene expression signature is associated with GSCs characterized by a restricted stem phenotype (Gsr lines), adherent growth, no CD133 expression and limited differentiation [58, 61, 62]. Consistently, by analysing the expression profiles of the 9 GSCs and relative sub-clones isolated and characterized by Günter and colleagues (4 with Gsf phenotype and 5 with Gsr phenotype) we found that PATZ1 is significantly enriched in Gsf-GSCs compared with Gsr-GSCs (Figure 7C). The association of PATZ1 expression with CD133 expression was further confirmed by the analysis of two separate experimental datasets consisting of cell lines established from 7 GBMs, 2 oligoastrocytomas and 5 normal foetuses plus primary biopsies from 6 normal brains [28], and 8 fresh primary and non cultured GBMs [29], where *PATZ1* expression is highly correlated with that of *PROM1* (the gene encoding prominin-1/ CD133) (Figure 7D), and is significantly enriched in the CD133+ compared to the CD133- subpopulation (Figure 7E). Consistently, in these cells lines *PATZ1* also correlates with markers of oligodendrocyte precursor cells, including *SOX8*, *OLIG1*, *OLIG2*, and *NKX2.2*, and of the proneural phenotype, such as *DLL3*, *OLIG2* and *SOX2* (Supplementary Table 4). All together these results indicate that PATZ1 is preferentially expressed in GSCs in comparison with matched non-GSCs, and is particularly enriched in proneural*versus*mesenchymal subtype.

To validate the *in silico*results, we analyzed *PATZ1* expression in 6 GSCs (3 growing in adhesion and 3 growing as spheres in laminin-coated dishes) isolated from patients affected by GBM in comparison with matched non-stem tumor cells (Figure 8A). The results confirmed an enriched expression of *PATZ1* in stem *versus* non-stem matched samples ($P < 0.05$; Figure 8B). The differences do not reach the statistical significance if we consider each group (sphere forming and growing in adhesion GSCs) singularly, likely because of the low number of samples, but they have a trend to be higher in GSCs compared to matched non-stem tumor cells (data not shown). Moreover, *PATZ1* expression was also analyzed in 5 more GBM-derived GSCs, for a total of 11 GSCs, which were sub-divided in two groups on the basis of their growth capacity in laminin-coated dishes (sphere/adherent). As shown in Figure 8C, and consistently with data shown in Figure 3C, *PATZ1* expression was highly enriched in GSCs growing as spheres compared to GSCs growing adherent ($P < 0.01$). All isolated GSCs, independently from their modality to grow in laminin-coated dishes, expressed markers of stemness, as confirmed by immunofluorescence analysis (Figure 8D), at higher levels compared with matched DIFF cells (data not shown). Immunofluorescence analysis confirmed expression of PATZ1 in GSC growing either as spheres

or in adhesion and their colocalizationwith the stemness marker Nestin (Figure 8E and data not shown). PATZ1 expression here appears mainly nuclear but a speckled cytosolic expression can be observed as previously described in other cancer cell types [27,51]. We also used the GBM cell lines U87MG to isolate GSC and analyze PATZ1 expression in comparison with matched bulk and differentiated cells (Supplementary Figure 1). PATZ1 protein expression resulted enriched in GSC *versus* both bulk and differentiated matched cells and correlated with expression of platelet-derived growth factor receptor β (PDGFRβ), a stem cell-specific marker in human GBM [63].

To further confirm *in vivo* the association of PATZ1 with the stem cell compartment of the GBM, we performed immunofluorescence labeling with antibodies anti-PATZ1 and GSC markers, including NESTIN and OCT-4, in 5 GBMs positive for PATZ1 expression. As shown in Figure 9, PATZ1 (red nuclear signal) was co-expressed with NESTIN (green cytoplasmic signal) in a sub-population of neoplastic cells. In these cells co-localization of OCT-4 (green nuclear signal) with PATZ1 was also evident.

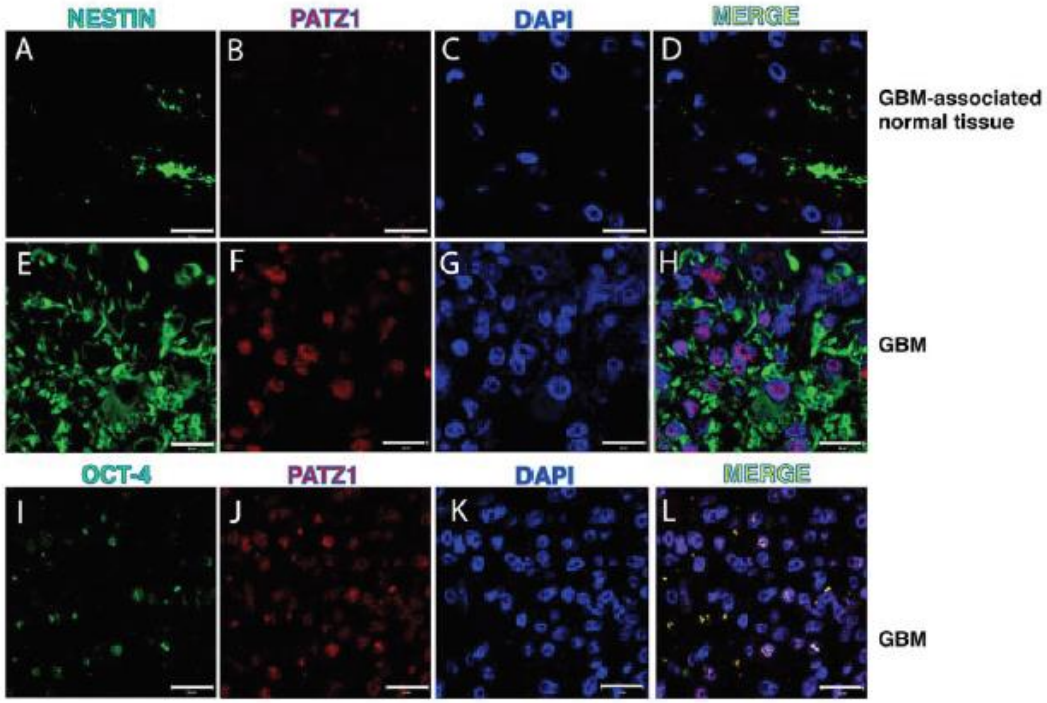

Figure 9: PATZ1 localization in the stem cell compartment of GBM. Representative confocal microscopy images of GBM (two samples with high PATZ1 score (+++) and GBM-associated normal tissues stained with anti-NESTIN **(A,E)**, antiOCT4 **(I)** and antiPATZ1 **(B,F,J)**. **(D, H, L)** Merge images showing co-localization of PATZ1 with either NESTIN or OCT-4. Scale bar: 20 µm

3. PATZ1 expression levels predict survival of GBM patients

The proneural GBM subtype is characterized by a trend toward longer survival, but is totally unresponsiveto aggressive treatment with concurrent chemo- and radiotherapy [7]. Consistent with the enrichment of PATZ1 in the proneural subtype, we showed in our local cohort of gliomas, that patients with low PATZ1 score (0/+) had a worse overall survival (OS) than patients with high PATZ1 score (++/+++) (HR = 2.525, 95% CI = 1.208- 5.280, p = 0.0138) (Figure 10A). The median OS for 16 patients with high PATZ1 was 36 months, in contrast to 12 months for 28 patients with low or absent PATZ1. Similarly, when we extended survival analyses to a larger cohort of GBM samples (n = 85), in which all subtypes were similarly represented (GBM – TCGA - 540), both OS and progression-free survival (PFS) were significantly correlated to PATZ1 expression, being worse in patients expressing low levels of PATZ1 (Supplementary Figure 2). In this same cohort of samples proneural GBMs have longer survival compared with mesenchymal subtype (Supplementary Figure 2, Panel C). Interestingly, also when we restricted the analysis to the proneural subset of GBM, Kaplan Meyer survival curves, followed by log-rank test, showed that PATZ1 expression stratifies these patients (n = 24) in two statistically different subgroups where low PATZ1 has worse OS (HR = 3.191, 95% CI = 2.355-14.31, p = 0.001) and PFS (HR = 3.595, 95% CI = 2.785-19.06, p = 0.0006) (Figure 10B–10C). The median OS for 10 patients with high *PATZ1* expression was 53 months, in contrast to 10 months for 14 patients with low *PATZ1*. Even more strikingly, the median PFS for patients with high *PATZ1* was 63 months *versus* 6 months for patients with low *PATZ1*. Moreover, the 5-year PFS was about 40% for proneural GBM patients with high *PATZ1* versus 0 with low *PATZ1*. In the same group of patients, using a multivariate Cox regression analysis, including known prognostic factors, such as age at diagnosis and methylation of the MGMT gene, low expression of PATZ1 resulted an independent prognostic factor for OS survival (HR= 0.2886, 95% CI = 0.0982-0.8482, p = 0.0246) and PFS (HR = 0.2458, 95% CI = 0.0802-0.7534, p = 0.0146).

These data suggest that PATZ1 expression has a crucial impact on outcome of GBM patients with a proneural classification, and could be used as an independent prognostic marker to predict survival and response to treatment.

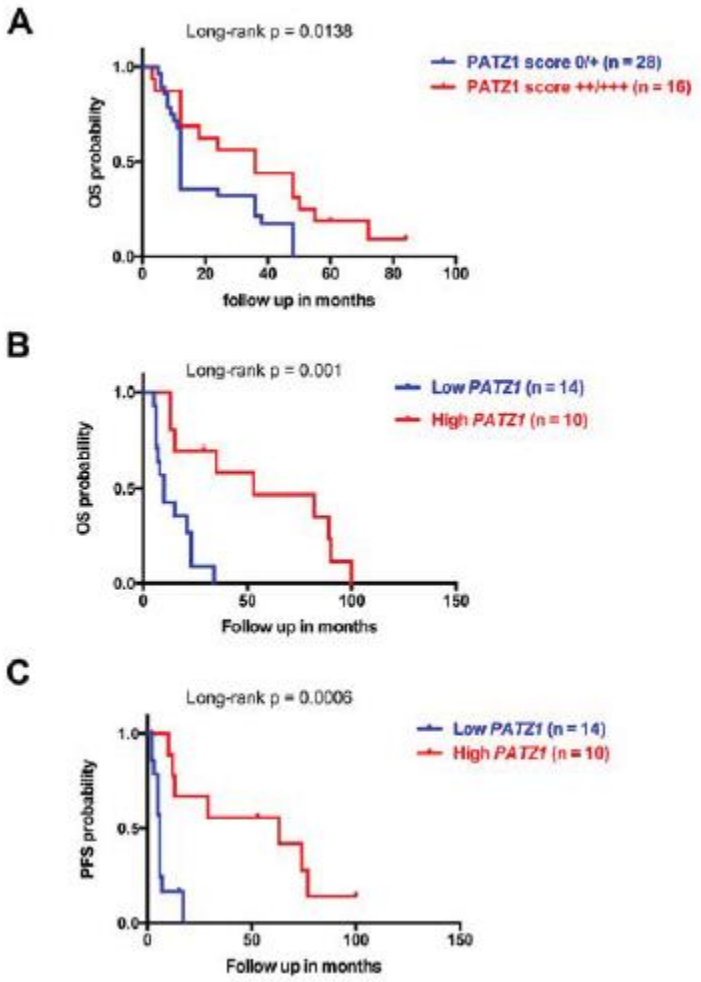

Figure 10: PATZ1 expression negatively correlates with survival in GBM patients. (A) Overall (OS) Kaplan-Meier survival curves of GBM patients shown in Suppelmentary Table 1, stratified by protein levels of PATZ1, as indicated. **(B)** OS and **(C)** Progression-Free (PFS) Kaplan-Meier curves of the proneural subset of GBM patients form the TCGA dataset shown in Figure 4B. Note that patients with lower PATZ1 expression have a worse survival rate than patients with higher PATZ1 as assessed by Log-Rank test

4. PATZ1 downregulates*CXCR4* expression in GBM

Remarkably, low PATZ1 samples shown in Figure 6B and 6C were mostly characterized (11 out of 14) by increased expression of the G-protein coupled receptor CXCR4 (Supplementary Table 5), which has been shown to induce and assist in the maintenance of a mesenchymal expression profile in GBM cells [64] and is overexpressed in CD133+ cells from human GBMs resistant to chemotherapy [65]. Indeed, we found that CXCR4 was a high significant prognostic and predictive factor in proneural GBM, were high CXCR4 patients show a worstoutcome considering both OS and PFS survival curves (Figure 11A–11B), and negatively correlated with PATZ1 in these patients ($r = -0.449$; $p = 0.03$) (Figure 11C). A similar negative correlation between PATZ1 and CXCR4 was also observed in GSCs (Supplementary Figure 3).

In order to investigate a possible role of PATZ1 in downregulating*CXCR4* gene expression in GBM cells, we transiently transfected the VS-GB cells, a GBM-derived primary cell line that does not express PATZ1, with a plasmid expressing PATZ1, and measured *CXCR4* mRNA and protein levels by qRT-PCR and western blot, respectively (Figure 11D). A significant decrease of both mRNA and protein levels was observed in cells expressing PATZ1 compared to empty vector-transfected control, supporting an inhibitory role of PATZ1 on CXCR4 expression. This is consistent with data extracted from the Trafac homology server, showing that the CXCR4 promoter harbor consensus sequence for PATZ1 [66], and with data extracted by our previous analysis of Patz1-knockout mouse embryonic fibroblasts [67], showing that Patz1-null mouse embryonic fibroblasts express a 4-fold change increase of Cxcr4 compared to wild-type littermate controls.

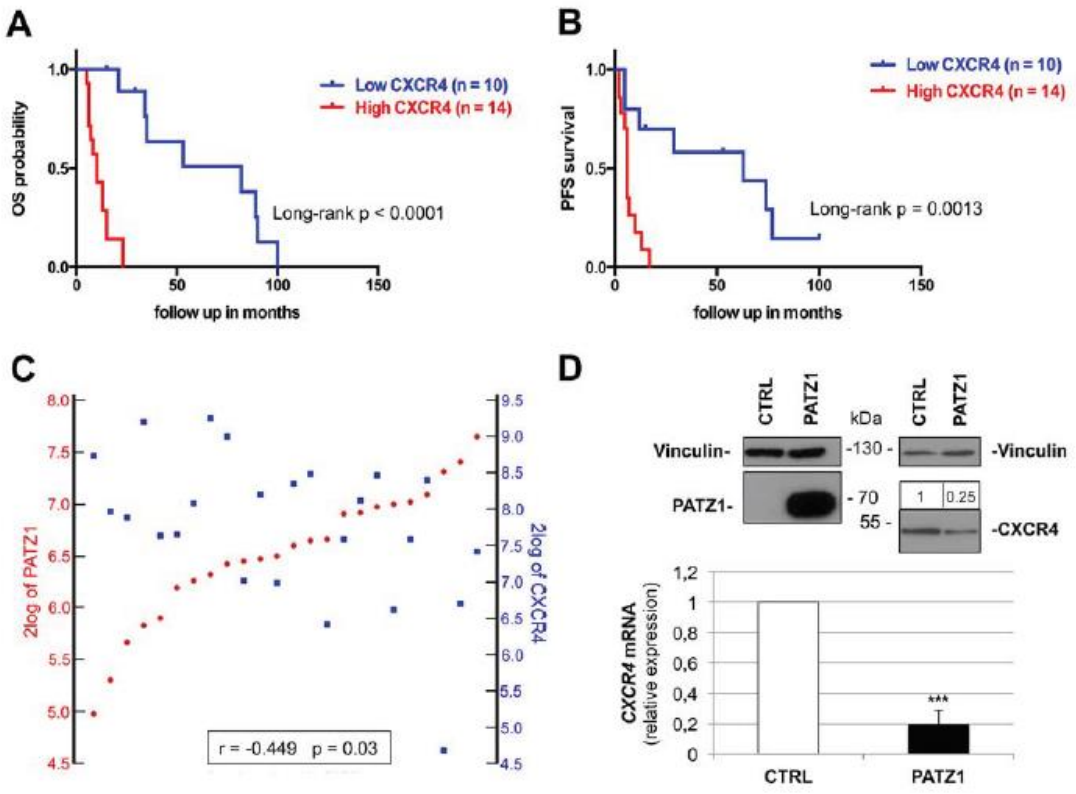

Figure 11: CXCR4 expression correlates positively with survival and negatively with PATZ1 in proneural GBM patients. (A) Overall survival (OS) and **(B)** Progression- Free survival (PFS) Kaplan-Meier curves of the patients shown in Figure 7B-7C (proneural subset of the TCGA dataset of GBM). Note that patients with higher *CXCR4* expression have worse survival rates than patients with lower *CXCR4*, as assessed by Log-Rank test. **(C)** YY-plots correlating PATZ1 and CXCR4 expression in the proneural GBMs shown in A and B. Significance of correlation (inbox) was analyzed by Pearson's χ^2 test through the R2 web platform (http://r2.amc.nl). **(D)** VS-GB cells were transiently transfected with 10 μg PATZ1 expressing plasmid, and endogenous CXCR4 mRNA was measured 48h later by qRT-PCR. CXCR4 mRNA levels were normalized for endogenous β-actin levels. The mean ±SE of three independent experiments, each in duplicate, is reported ***, P=0.0001. PATZ1 and CXCR4 protein expression is shown on the top by western blot analysis, using vinculin detection as a loading control.

Densitometric analysis by Image J software was applied: relative expression levels of CXCR4, compared to empty vector-transfected control and normalized with respect to vinculin, are indicated on the top of the blot.

DISCUSSION

One of the most important hallmarks of GBM is the marked heterogeneity within and across these tumors, which has been attributed to cancer cell plasticity [68]. According to the cancer stem-cell model some cancers are organized into a hierarchy of subpopulations of tumorigenic cancer stem cells, which drive tumor growth, therapy resistance and disease progression. It is therefore imperative to clarify the markers that can be used to identify these cells and the context in which they work [69]. It has been recently proposed that patient-derived glioblastoma stem-like cells (GSCs) can be sub-divided in two main groups, one characterized by a proneural-like phenotype and the other showing a mesenchymal-like phenotype according to the molecular subtype classification of the TCGA [7,61]. Phenotypically, proneural GSCs exhibit non-adherent sphere forming growth *in vitro* and circumscribed, non-invasive growth *in vivo*. In contrast, mesenchymal cells grow semi-adherently *in vitro* and show invasive growth *in vivo* [61,70]. Accordingly, patients with proneural GBM have a trend toward longer survival [7], whereas patients with mesenchymal GBM show the worst outcome [71].

In this study we analyzed expression of the Kruppel-type Zinc Finger transcription factor PATZ1 in GBM and oligodedrogliomas, finding it was highly expressed in a significant number of cases, whereas it was undetectable in normal glia. Moreover, we showed that PATZ1 is expressed in GSCs both *in vitro* (in GBM-derived stem cells) and *in vivo* (human tissue specimens), is downregulated in differentiated cells from the same tumor as compared to GSCs, and its expression is higher in GSCs growing as spheres (likely proneural) than in GSCs growing as adherent cells (likely mesenchymal). These observations were validated and completed in independent glioma datasets, finding a significant overlap of high PATZ1 expression with the proneural subtype and conversely of low PATZ1 expression with the mesenchymal subtype in both GBMs and GSCs. Since PATZ1 has been described as an inhibitor of cell proliferation in some cancer cell contexts [13,27,72], we would expect that GSCs growing as spheres that express higher levels of PATZ1 compared to GSCs growing in adhesion may proliferate less. However, sincethere are no differences in the proliferation rate between GSCs growing as spheres and those growing as adherent cells [58], we concluded that PATZ1 is not associated with proliferation in these cells. Interestingly, confocal microscopy analysis of human GBM specimens showed that PATZ1 was expressed in the NESTIN+ subpopulation, which has been recently shown to be crucial for tumor recurrence after treatment with the chemotherapeutic agent temozolomide[32].

Finally, we characterized the prognostic impact of PATZ1 expression first in our local cases of GBM,finding a significant worst outcome in patients showing absent or low levels of PATZ1

(<10% positive cells), suggesting it may be used as a prognostic marker. Then, extending the analysis to the TCGA dataset, including samples subclassified in the four subtypes described by Verhaak et al. [7], the capacity of PATZ1 to discriminate GBM patients with different prognosis was significantly shown also in the proneural subtype, where low levels of PATZ1 correlate with a worst outcome in both overall and progression-free survival curves, independently from other known prognostic factors, such as MGMT promoter methylation and age at diagnosis. Therefore, despite PATZ1 is enriched in the proneural subtype, there are proneural GBMs that express low levels of PATZ1 that are associated with a shorter patients survival. This is consistent with the already described intra-subtype heterogeneity of GBMs, which highlights the importance of finding new markers able to further sub-classify each subtype [68].

Since PATZ1 loss/downregulation has been associated with the acquisition of a mesenchymal phenotype in cancer cells [27], and the mesenchymal phenotype in GBMs is associated with the poorest prognosis and most aggressive phenotype, with advantage in proliferative capacity and neovascularization [71,73], we speculate that a subset of proneural GBMs may be more aggressive due to the downregulation of PATZ1 and consequent activation of a mesenchymal program. Consistent with this hypothesis, we found that in the proneural subset there was a 75% of negative concordance ($r = -0.44$; $p = 0.03$) between PATZ1 and CXCR4, whose overexpression is an outcome common to multiple mechanisms of Epithelial-Mesenchymal Transition (EMT) induction in GBM and directly involved in determining the EMT phenotype [74]. Interestingly, according to the Trafac homology server, the CXCR4 promoter harbors consensus sequence for PATZ1 [66], and Patz1-null mouse embryonic fibroblasts express a 4-fold change increase of Cxcr4 compared to wild-type littermate controls [67]. Therefore, it is possible that PATZ1 could be directly involved in CXCR4 silencing. Indeed, it has been hypothesized that factors associated with the more stem-like phenotype may account for CXCR4 expression in GBM [62], and we provided evidence that PATZ1 could be one of these factors: in VS-GB cells, a primary GBM cell line that does not express endogenous PATZ1, overexpression of PATZ1 leads to downregulation of CXCR4. Further experiments are ongoing in our laboratory to explore the possibility of a direct role of PATZ1 on the CXCR4 promoter in GBM as well as in other cancer-derived cell lines, where PATZ1 appears involved in counteracting EMT. According to current opinions envisaging a parallel between dedifferentiation of cancer cells and reprogramming of somatic cells [75], the transdifferentiation of tumor cells from proneural to mesenchymal may imply a reprogramming process thatleads differentiated cells to reacquire the capacity to differentiate into different cells. This is consistent with our previous results showing that PATZ1 plays an inhibitory role in the reprogramming process [67], and suggests a potential PATZ1 inhibitory role on the transition from the mesenchymal to the proneuralphenotype.

However, further functional experiments are needed to demonstrate the involvement of the PATZ1-CXCR4 axis in the proneural-to-mesenchymalphenotipic switch.

In conclusion, we describe PATZ1 as a novel biomarker of GBM and GSCs, differentially expressed among GBM and GSC subtypes and able to further subdivide the proneural GBM subtype in two populations with different overall and progression free survival. As PATZ1 has been proven an important transcription factor involved in stem cell pluripotency[76], it is encouraging to see that the proneural type of GBM, characterized by a stem-like signature, has higher expression of PATZ1 compared to other types. Finally, this finding may explain the paradox that the proneural type of GBM resist standard therapeutic caused by the cancer stem cells maintained by PATZ1 involved transcription factor networks while at the same time PATZ1 restrict the proneural type of GBM to differentiation into mesenchymal type.

REFERENCES

1. CBTRUS. Statistical Report: Primary Brain Tumors in the United States in 2007-2011. Published by Oxford University Press on behalf of the Society for Neuro-Oncology in cooperation with the Central Brain Tumor Registry 2014
2. Crocetti E, Trama A, Stiller C et al. Epidemiology of glial and non-glial brain tumours in Europe. *Eur J Cancer*. 2012 Jul;48(10):1532-42
3. Ferlay J, Soerjomataram I, Ervik M, et al. GLOBOCAN 2012 v1.0, Cancer Incidence and Mortality Worldwide: IARC CancerBase No. 11 [Internet]. Lyon, France: International Agency for Research on Cancer; 2013. Available from: http://globocan.iarc.fr, accessed December 2013
4. David N. Louis, Arie Perry, Guido Reifenberger, Andreas von Deimling, Dominique Figarella-Branger, Webster K. Cavenee, Hiroko Ohgaki, Otmar D. Wiestler, Paul Kleihues, David W. Ellison. The 2016 World Health Organization Classification of Tumors of the Central Nervous System: a summary. ActaNeuropathol 2016, 131:803-820
5. Louis DN, Ohgaki H, Wiestler OD, Cavenee WK. WHO Classification of Tumors of the Central Nervous System. Lyon: International Agency for Research; 2007
6. Andrew Morokoff, Wayne Ng, Andrew Gogos, Andrew H. Kaye. Molecular subtypes, stem cells and heterogeneity: implications for personalised therapy in glioma. Journal of Clinical Neuroscience 22 (2015) 1219-1226
7. Verhaak RG, Hoadley KA, Purdom E, Wang V, Qi Y, Wilkerson MD, Miller CR, Ding L, Golub T, Mesirov JP ET AL. Integrated genomic analysis identifies clinically relevant subtypes of glioblastoma characterized by abnormalities in PDGFRA, IDH1, EGFR, and NF1. Cancer Cell 2010; 17: 98-110
8. Fedele M, Benvenuto G, Majello B et al. A novel member of the BTB/POZ family, PATz1, associates with the RNF4 RING finger protein and acts as a transcriptional repressor. *J BiolChem* 275: 7894-7901
9. Klug A, Schwabe JW. Protein motifs 5. Zinc Fingers. FASEB J 1995; 9: 597-604
10. Restifo LL and White K. Mutations in a steroid hormone-regulated gene disrupt the metamorphosis of the central nervous system in Drosophila*. Dev. Biol*. 1991; 148: 174-194
11. Karim FD et al. The Drosophila broad-complex plays a key role in controlling ecdysone-regulated gene expression at the onset of metamorphosis. *Development* 1993; 118: 977-988
12. Sahut- Barnola I et al. *Drosophila* ovary morphogenesis: analysis of terminal filament formation and identification of a gene required for this process. *Dev Biol*1995; 170: 127-135

13. Valentino T, Palmieri D, Vitiello M, et al. Embryonic Defects and Growth alteration in Mice With Homozygous Disruption of the Patz1 Gene. J Cell Physiol 2013; 228 (3): 646-53
14. Kobayashi A, Yamagiwa H, Hoshino H et al. A combinatorial code for gene expression generated by transcription factor Bach2 and MAZR (MAZ-related factor) through the BTB/POZ domain. *Mol Cell Biol* 2000; 20: 1733-1746
15. Lombardi Z, Tiffin N, Hofman O et al. Computational selection and priorization of candidate genes for fetal alcohol syndrome. *BMC Genomics* 2007; 8; 389
16. Fedele M, Franco R, Salvatore G, et al. PATZ1 gene has a critical role in the spermatogenesis and testicular tumours. *J Pathol* 2008; 215: 39-47
17. Mastrangelo T, Modena P, Tornielli S et al. A novel zinc finger gene is fused to EWS in small round cell tumor. *Oncogene* 2000; 19: 3791-3804
18. Tritz R, Mueller BM, Hickey MJ, et al. siRNA Down-regulation of the PATZ1 Gene in Human Glioma Cells Increases Their Sensitivity to Apoptotic Stimuli. *Cancer Ther* 2008; 6(B): 865-876
19. Muschen M, re D, Betz B et al. Resistance to CD95-mediated apoptosis in breast cancer is not due to somatic mutation of the CD95 gene. *Int J Cancer* 2001; 92: 309-10
20. Riffkin CD, Gray AZ, Hawkins CJ et al. Ex vivo pediatric brain tumors express Fas (CD95) and FasL (CD95L) and are resistant to apoptosis induction. Neuro-oncol 2001; 3: 229-40
21. Barnhart BC, Legembre P, Pietras E et al. CD95 ligand induces motility and invasiveness of apoptosis-resistant tumor cells. EMBO J 2004; 23: 3175-85
22. Yang B, Lin H, Hor W. Mediation of enhanced transcription of the IL10 gene in T cells, upon contact with human glioma cells, by Fas signaling through a protein kinase A-indipendent pathway. J Immunol 2003; 171: 3947-54
23. Gomez GG, Kruse CA. Mechanisms of malignant glioma immune resistance and sources of immunosoppression. *Gene TherMolBiol* 2006; 10: 133-46
24. Merlo A. Genes and pathways driving glioblastomas in humans and murine disease models. *Neurosurg Rev* 2003; 26: 145-58
25. Viglietto G, Motti ML, Bruni P, et al. Cytoplasmic relocalization and inhibition of the cyclin-dependent kinase inhibitor p27Kip1 by PKB/Akt-mediated phosphorylation in breast cancer. *Nat Med* 2002; 8: 1131-1144
26. Tian X, Sun D, Zhang Y, Zhao S, Xiong H, Fang J. Zinc finger protein 278, a potential oncogene in human colorectal cancer.*Acta BiochimBiophys Sin (Shanghai)* 2008 Apr;40(4):289-96

27. Chiappetta G, Valentino T, Vitiello M et al. PATZ1 acts as a tumor suppressor in thyroid cancer via targeting p53-dependent genes involved in EMT and cell migration. Oncotarget 2015; vol6 (7): 5310-5323
28. Borovski T, De Sousa e Melo F, Vermeulen L et al. Cancer stem cell niche: the place to be, *Cancer Res*. 2011; 71: 634-639
29. Brabletz S, Schmalhofer O, Brabletz T. Gastrointestinal stem cells in development and cancer. J Pathol 2009; 217: 307-317
30. Jin L, Hope KJ, Zhai Q et a. Targeting of CD44 eradicates human acute myeloid leukemic stem cells. Nat Med 2006; 12: 1167-74
31. Ito K, Bernardi R, Morotti A et al. PML targeting eradicates quiescent leukaemia-initiating cells. Nature 2008; 453: 1072-8
32. Chen J, Li Y, Yu TS et al. A restricted cell population propagates glioblastoa growth after chemotherapy. Nature 2012; 488: 522-6
33. Ow JR, Ma H, Jean A et al. Patz1 regulates embryonic stem cell identity. *Stem Cells Dev* 2014; 23: 1062-73
34. Evans MJ, Kaufman MH. Establishment in culture of pluripotential cells from mouse embryos. Nature 1981; 292:154-156
35. Martin GR. Isolation of a pluripotent cell line from early mouse embryos cultured in medium conditioned by teratocarcinoma stem cells. Proc Natl AcadSci USA 1981; 78: 7634-7638
36. Nichols J, Davidson D, Taga T et al. Complementary tissue-specific expression of LIF and LIF-receptor mRNAs in early mouse embryogenesis. *Mech Dev* 1996; 57: 123-131
37. Ying QL, Nichols J, Chambers I et al. BMP induction of Id proteins proteins suppresses differentiation and sustains embryonic stem cells self-renewal in collaboration with STAt3. *Cell* 2003; 115: 281-292
38. Stato N, Meijer L, Skaltsounis L et al. Maintenance of pluripotency in human and mouse embryonic stem cells through activation of Wnt signaling by a pharmacological GSK-3-specific inhibitor. *Nat Med* 2004; 10: 55-63
39. Xu RH, Peck RM, Li DS et al. Basic FGF and suppression of BMP signaling sustain undifferentiated proliferation of human ES cells: *Nat Methods* 2005; 2: 185-190
40. Liu X, Huang J, Chen T, et al. Yamanaka factors critically regulate the developmental signaling network in mouse embryonic stem cells. *Cell Res* 2008; 18 (12); 1177-89
41. Yoshikawa T, Piao Y, Zhong J et al. High-throughput screen for genes predominantly expressed in the ICM of mouse blastocysts by whole mount in situ hybridization. *Gene Expr Patterns* 2006; 6: 213-224

42. Tang F, Barbacioru C, Bao S, et al. Tracing the derivation of embryonic stem cells from the inner cell mass by single-cell RNA-Seq analysis. *Cell Stem Cell* 2010; 6: 468-478
43. Kim J, Chu J, Shen X et al. An extended transcriptional network for pluripotency of embryonic stem cells. *Cell* 2008; 132: 1049-1061
44. Nishiyama A, Xin L, Sharov AA et al. Uncovering early response of gene regulatory network in ESCs by systematic induction of transcription factors. *Cell Stem Cell* 2009; 5: 420-433
45. Ow JR, Ma H, Jean A et al. Patz1 Regulates Embryonic Stem Cel Identity. Stem Cells and Development 2014; 23 (10): 1062-1073
46. Temple S. The development of neural stem cells. *Nature* 2001, 414: 112-117
47. Buaas WF, Kirsh AL, Sharma M et al. Plzf is required in adult male germ cells for stem cell self-renewal. *Nat Genet* 2004; 36:641-652
48. Costoya JA, Hobbs RM, Barna M et al. Essential role of Plzf in maintenance of spermatogonial stem cells. *Nat Genet* 2004; 36: 651-659
49. Gaspar-Maia A, Alajem A, Meshorer E et al. Open chromatin in pluripotency and reprogramming. *Nat Rev Mol Cell Biol* 2011; 12: 36-47
50. Ma Hui, Ow JR, Peow an , et al. The dosage of patz1 modulates reprogramming process. *Scientific reports* 2014; 4: 7519
51. Franco R, Scognamiglio G, Valentino E, Vitiello M, Luciano A, Palma G, Arra C, La Mantia E, Panico L, Tenneriello V, Pinto A, Frigeri F, Capobianco G, et al. PATZ1 expression correlates positively with BAX and negatively with BCL6 and survival in human diffuse large B cell lymphomas. Oncotarget. 2016; 7:59158-59172
52. Calì G, Gentile F, Mogavero S, Pallante P, Nitsch R, Ciancia G, Ferraro A, Fusco A, Nitsch L. CDH16/Ksp-cadherin is expressed in the developing thyroid gland and is strongly down-regulated in thyroid carcinomas. Endocrinology. 2012; 153:522-534
53. Andolfi L, Bourkoula E, Migliorini E, Palma A, Pucer A, Skrap M, Scoles G, Beltrami AP, Cesselli D, Lazzarino M. Investigation of adhesion and mechanical properties of human glioma cells by single cell force spectroscopy and atomic force microscopy. PLoS One. 2014; 9:e112582.
54. Bourkoula E, Mangoni D, Ius T, Pucer A, Isola M, Musiello D, Marzinotto S, Toffoletto B, Sorrentino M, Palma A, Caponnetto F, Gregoraci G, Vindigni M, et al. Glioma-associated stem cells: a novel class of tumor-supporting cells able to predict prognosis of human low-grade gliomas. StemCells. 2014; 32:1239-1253
55. Camorani S, Esposito CL, Rienzo A, Catuogno S, Iaboni M, Condorelli G, de Franciscis V, Cerchia L. Inhibition of receptor signaling and of glioblastoma-derived tumor growth by a novel PDGFRβ aptamer. Mol. Ther. 2014; 22: 828-841.

56. Livak KJ, Schmittgen TD. Analysis of relative gene expression data using real-time quantitative PCR and the 2(-Delta Delta C(T)) Method. Methods. 2001; 25:402-408.
57. French PJ, Peeters J, Horsman S, Duijm E, Siccama I, van den Bent MJ, Luider TM, Kros JM, van der Spek P, SillevisSmitt PA. Identification of differentially regulated splice variants and novel exons in glial brain tumors using exon expression arrays. Cancer Res. 2007; 67:5635-5642
58. Günter HS, Schmidt NO, Phillips HS, Kemming D, Kharbanda S, Soriano R, Modrusan Z, Meissner H, Westphal M, Lamszus K. Glioblastoma-derived stem cell-enriched cultures form distinct subgroups according to molecular and phenotypic criteria. Oncogene 2008; 27:2897-2909.
59. Pollard SM, Yoshikawa K, Clarke ID, Danovi D, Stricker S, Russell R, Bayani J, Head R, Lee M, Bernstein M, Squire JA, Smith A, Dirks P. Glioma stem cell lines expanded in adherent culture have tumor-specific phenotypes and are suitable for chemical and genetic screens. Cell Stem Cell. 2009;4:568-580
60. Garcia JL, Perez-Caro M, Gomez-Moreta JA, Gonzalez F, Ortiz J, Blanco O, Sancho M, Hernandez-Rivas JM, Gonzalez- Sarmiento R, Sanchez-Martin M. Molecular analysis of ex-vivo CD133+ GBM cells revealed a common invasive and angiogenic profile but different proliferative signatures among high grade gliomas. BMC Cancer. 2010;10:454
61. Marziali G, Signore M, Buccarelli M, Grande S, Palma A, Biffoni M, Rosi A, D'Alessandris QG, Martini M, Larocca LM, De Maria R, Pallini R, Ricci-Vitiani L. Metabolic/ ProteomicSignatureDefinesTwo Glioblastoma Subtypes With DifferentClinicalOutcome. Sci Rep. 2016; 6:21557
62. Schulte A. Gunther HS, Phillips HS, Kemming D, Martens T, Kharbanda S, Soriano RH, Modrusan Z, Zapf S, Westphal M, Lamszus K. A distinct subset of glioma cell lines with stem cell-like properties reflects the transcriptional phenotype of glioblastomas and overexpresses CXCR4 as therapeutic target. Glia. 2011; 59:590-602
63. Kim Y, Kim E, Wu Q, Guryanova O, Hitomi M, Lathia JD, SerwanskiD,Sloan AE, Weil RJ, Lee J, Nishiyama A, Bao S, Hjelmeland AB, et al. Platelet-derived growth factor receptors differentially inform intertumoral and intratumoral heterogeneity. GenesDev. 2012; 26:1247-1262
64. Zhu Y, Yang P, Wang Q, Hu J, Xue J, Li G, Zhang G, Li X, Li W, Zhou C, Zhao M, Wang D. The effect of CXCR4 silencing on epithelial-mesenchymal transition related genes in glioma U87 cells. Anat Rec (Hoboken). 2013; 296:1850-1856
65. Liu G, Yuan X, Zeng Z, Tunici P, Ng H, Abdulkadir IR, Lu L, Irvin D, Black KL, Yu JS. Analysis of gene expression and chemoresistance of CD133+ cancer stem cells in glioblastoma.Mol Cancer. 2006; 5:67

66. Jegga AG, Sherwood SP, Carman JW, Pinski AT, Phillips JL, Pestian JP, Aronow BJ. Detection and visualization of compositionally similar cis-regulatory element clusters in orthologous and coordinately controlled genes. Genome Res. 2002; 12:1408-1417.
67. Ma H, Ow JR, Tan BC, Goh Z, Feng B, Loh YH, Fedele M, Li H, Wu Q. The dosage of Patz1 modulates riprogramming process. Sci Rep. 2014; 4:7519
68. Friedmann-Morvinski. Glioblastoma heterogeneity and cancer cell plasticity. CritRevOncog. 2014; 19:327-336.
69. Meacham CE, Morrison SJ. Tumour heterogeneity and cancer cell plasticity. Nature. 2013; 501:328-337
70. Brown DV, Daniel PM, D'Abaco GM, Gogos A, Ng W, Morokoff AP, Mantamadiotis T. Coexpression analysis of CD133 and CD44 identifies proneural and mesenchymal subtypes of glioblastoma multiforme. Oncotarget. 2015; 6:6267-6280
71. Kim YW, Koul D, Kim SH, Lucio-Eterovic AK, Freire PR, Yao J, Wang J, Almeida JS, Aldape K, Yung WK. Identification of prognostic gene signatures of glioblastoma: a study based on TCGA data analysis. Neuro Oncol. 2013;15:829-839
72. Vitiello M, Valentino T, De Menna M, Crescenzi E, Francesca P, Rea D, Arra C, Fusco A, De Vita G, Cerchia L, Fedele M. PATZ1 is a target of miR-29b thatisinduced by Ha-Ras oncogene in ratthyroidcells. Sci Rep. 2016; 6:25268
73. Phillips HS, Kharbanda S, Chen R, Forrest WF, Soriano RH, Wu TD, Misra A, Nigro JM, Colman H, Soroceanu L, Williams PM, Modrusan Z, Feuerstein BG, et al. Molecular subclasses of high-grade glioma predict prognosis, delineate a pattern of disease progression, and resemble stages in neurogenesis. Cancer Cell. 2006; 9:157-173
74. Richardson PJ. CXCR4 and Glioblastoma. Anticancer Agents MedChem. 2016; 16:59-74
75. Friedmann-Morvinski D, Verma IM. Dedifferentiation and reprogramming: origins of cancer stem cells. EMBO Rep. 2014; 15:244-253
76. Ow JR, Ma H, Jean A, Goh Z, Lee YH, Chong YM, Soong R, Fu XY, Yang H, Wu Q. Patz1 regulates embryonic stem cell identity. Stem Cells Dev. 2014; 23:1062-1073

SUPPLEMENTARY MATERIALS

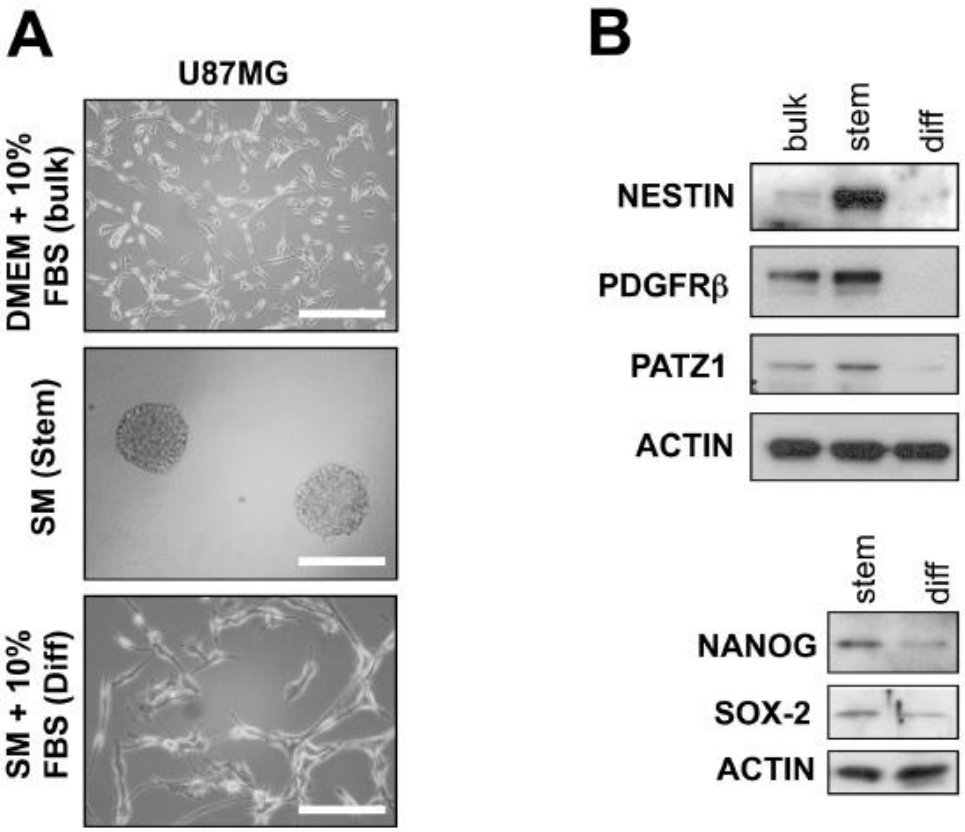

Supplementary Figure 1: PATZ1 in U87MG cells growing as spheres

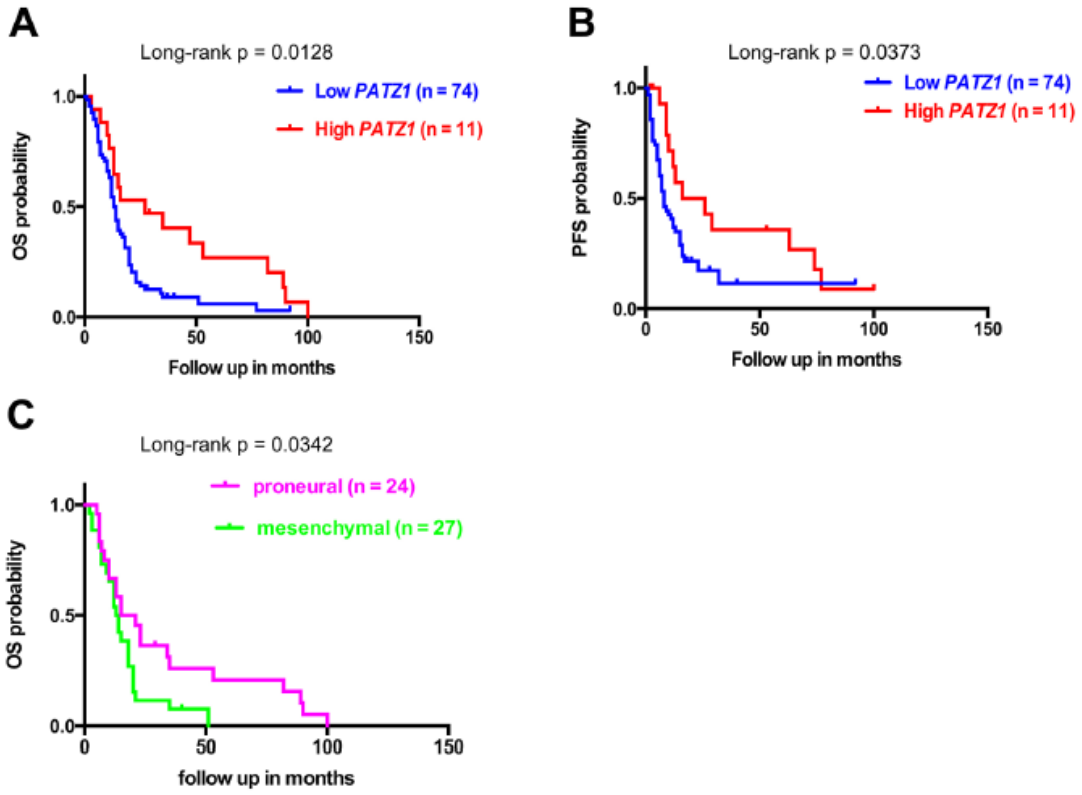

Supplementary Figure 2: Survival curves in GBM patients from the TCGA dataset

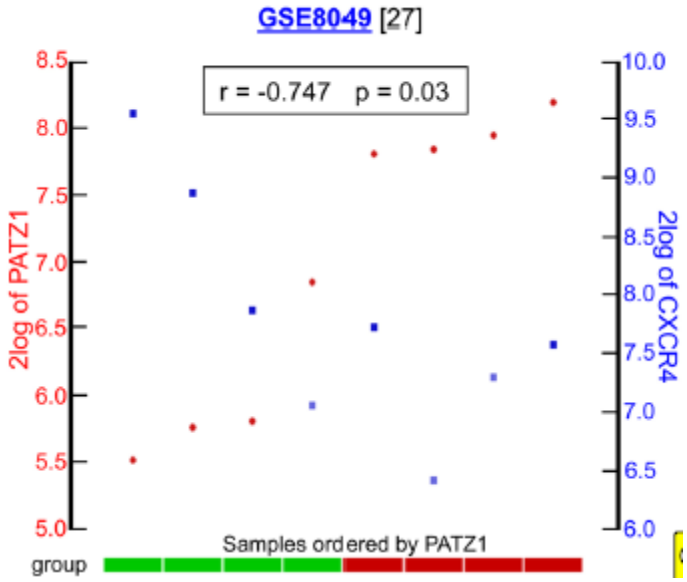

Supplementary Figure 3: *PATZ1/CXCR4* correlation in GSCs

Case	Gender	Age	Site	PATZ1
1	F	71	f	-
2	F	62	t	-
3	M	70	t	+
4	F	66	t	++
5	M	35	p	++
6	M	65	t	-
7	F	69	t	-
8	F	41	f	+
9	F	58	f	+
10	M	64	t	+++
11	F	64	t	++
12	M	72	t	+
13	M	58	f	+
14	M	74	t	+
15	M	62	t	-
16	F	44	c	-
17	F	64	p	-
18	M	62	t	++
19	M	60	t	+
20	M	65	f	-
21	M	57	f	+
22	M	66	p	++
23	F	36	t	++
24	M	62	o	+
25	M	62	t	+
26	M	63	o	+
27	M	69	t	+++
28	F	26	p	++
29	M	73	t	-
30	F	72	t	++
31	M	73	p	+++
32	M	70	p	-
33	M	52	t	+++
34	M	41	t	++
35	M	63	p	++
36	M	60	p	++
37	M	61	t	-
38	M	64	p	+
39	M	69	p	+++
40	F	81	p	+
41	F	75	f	-
42	M	54	f	+
43	M	68	t	+
44	M	74	f	+
45	F	72	t	-

f, frontal; t, temporal; o, occipital; p, parietal; c, corpus callosum

Supplementary Table 1: Clinicopathological features and PATZ1 expression of 45 glioblastomas (local cohort analyzed by IHC)

Case	Gender	Age	Site	Grade	PATZ1
1	M	66	t	III	+
2	F	67	f	II	-
3	M	44	f	II	-
4	F	50	t	II	-
5	F	54	f	III	-
6	M	39	f	II	-
7	M	57	o	III	+
8	M	33	f	II	+++
9	M	26	f	II	-
10	M	58	o	III	+
11	M	31	f	II	-
12	M	35	f	II	++
13	F	54	t	III	++
14	M	69	f	III	++
15	M	69	o	III	++
16	F	38	t	III	-
17	M	41	i	III	+++
18	M	41	f	III	+++
19	F	43	f	II	++
20	F	40	f	II	+
21	M	77	f	II	-
22	M	22	f	II	-

f, frontal; t, temporal; o, occipital; p, parietal; i, intramedullary metastasis

Supplementary Table 2: Clinicopathological features and PATZ1 expression of 22 oligodendrogliomas (local cohort analyzed by IHC)

Gene	r[b]	p	gene	R	P
THBS1	-0.317	3.2e-13	*DAB2*	-0.270	8.1e-10
COL8A2	-0.317	3.4e-13	*TGOLN2*	-0.265	1.9e-09
LTBP1	-0.314	5.8e-13	*NRP1*	-0.262	2.9e-09
HFE	-0.305	2.8e-12	*LAPTM5*	-0.262	2.8e-09
LCP1	-0.305	3.1e-12	*NCF4*	-0.253	9.8e-09
TNFRSF1A	-0.302	5.1e-12	*COL1A2*	-0.251	1.5e-08
PDPN	-0.298	8.8e-12	*DSC2*	-0.250	1.6e-08
ADAM12	-0.297	1.2e-11	*CD44*	-0.242	4.6e-08
TNFRSF1B	-0.297	1.1e-11	*EFEMP2*	-0.241	5.6e-08
IL15RA	-0.294	1.9e-11	*COL5A1*	-0.241	5.2e-08
PLK3	-0.290	3.9e-11	*WWTR1*	-0.237	8.8e-08
ITGA5	-0.289	4.5e-11	*PTRF*	-0.236	1.0e-07
SLC11A1	-0.285	8.0e-11	*MVP*	-0.234	1.4e-07
TRADD	-0.280	1.8e-10	*PTPN6*	-0.231	2.0e-07
MAPK13	-0.278	2.4e-10	*MRC2*	-0.231	2.0e-07
CDCP1	-0.277	3.0e-10	*IL4R*	-0.228	3.0e-07
RAB11FIP1	-0.277	2.8e-10	*CDAP*	-0.225	4.6e-07
CLCF1	-0.276	3.6e-10	*HK3*	-0.223	5.6e-07
GCNT1	-0.276	3.2e-10	*FNDC3B*	-0.212	2.1e-06
LCP2	-0.275	4.2e-10	*DCBLD2*	-0.210	2.6e-06
FOLR2	-0.274	4.4e-10	*CNN2*	-0.207	3.9e-06
TNFRSF11A	-0.271	7.7e-10			

[a] All genes belong to the mesenchymal signature described by Verhaak et al. [7]

[b] Correlations were analyzed by Pearson's χ^2 test through the R2 platform (http://r2.amc.nl)

Supplementary Table 3: Other correlations between PATZ1 and the mesencymal signature in GBM[a]

	GSE8049 (Gunter et al. 2008)	GSE15209 (Pollard et al. 2009)
DLL3	r = 0.844; p = 2.1e-05	r = 0.56; p = 1e-02
SOX2	r = 0.617; p = 8.4e-03	r = 0.837; p = 4.2e-06
SOX8	r = 0.681; p = 2.6e-03	r = 0.704; p = 5.3e-04
NES	r = 0.655; p = 4.3e-03	r = 0.611; p = 4.2e-03
OLIG2	r = 0.739; p = 7.1e-04	r = 0.556; p = 1e-02
OLIG1	r = 0.687; p = 2.3e-03	r = 0.556; p = 1e-02
NKX2.2	r = 0.566; p = 2e-02	r = 0.494; p = 3e-03
DCX	r = 0.488; p = 5e-02	r = 0.705; p = 5.2e-04
ASCL1	r = 0.761; p = 3.9e-04	r = 0.778; p = 5.3e-05
TCF4	r = 0.577; p = 2e-02	r = 0.582; p = 7.1e-03

Supplementary Table 4: Oligodendrocyte precursor and proneural gene expression correlations with PATZ1 in GBM-derived stem cells

ID patient	OS f/u (months)	PFS f/u (months)	Age	MGMT methylation	*PATZ1* (Cutoff: 100.6)	*CXCR4* (Cutoff: 197.7)
02-0003[a]	5	5	50	No	Low	High
06-0648	10	7	77	Yes	Low	High
12-0618	13	2	49	No	High	High
06-0238	13	10	46	No	High	High
12-0616	15	13	36	No	High	High
02-0069	29	29	31	Yes	High	Low
02-0010	35	12	20	No	High	Low
02-0024	53	53	35	No	High	Low
02-0014	82	74	25	No	High	Low
02-0080	89	77	28	No	High	Low
02-0028	90	63	39	Yes	High	Low
02-0114	100	100	37	Yes	High	Low
06-0646	6	3	60	No	Low	High
06-0166	6	2	51	No	Low	High
02-0060	6	6	66	No	Low	High
02-0046	7	6	61	No	Low	High
02-0058	8	6	28	Yes	Low	High
02-0074	10	5	68	No	Low	High
06-0241	15	15	66	Yes	Low	Low
02-0047	15	2	78	No	Low	High
02-0011	21	5	19	No	Low	Low
06-0128	23	6	66	No	Low	High
02-0007	23	17	40	No	Low	High
06-0129	34	5	30	No	Low	Low

[a] samples highlighted in gray show opposite expression levels of *PATZ1* and *CXCR4* (75% negative concordance)

Supplementary Table 5: Molecular and clinical features in proneural GBM (TCGA dataset)